

# Production and purification of fungal enzymes

---

Zrilić, Matea

Master's thesis / Diplomski rad

2020

Degree Grantor / Ustanova koja je dodijelila akademski / stručni stupanj: **University of Zagreb, Faculty of Food Technology and Biotechnology / Sveučilište u Zagrebu, Prehrambeno-biotehnološki fakultet**

Permanent link / Trajna poveznica: <https://um.nsk.hr/um:nbn:hr:159:597355>

Rights / Prava: [Attribution-NoDerivatives 4.0 International](#)/[Imenovanje-Bez prerada 4.0 međunarodna](#)

Download date / Datum preuzimanja: **2024-11-18**



Repository / Repozitorij:

[Repository of the Faculty of Food Technology and Biotechnology](#)



UNIVERSITY OF ZAGREB  
FACULTY OF FOOD TECHNOLOGY AND BIOTECHNOLOGY

# GRADUATE THESIS

Zagreb, July 2020.

Matea Zrilić  
1153/BPI

**PRODUCTION AND  
PURIFICATION OF FUNGAL  
ENZYMES**

Experimental work for this Graduate thesis was done at Department of Food Science and Technology, BOKU – University of Natural Resources and Life Science, Vienna. The thesis was made under the guidance of associate professor Roland Ludwig, Ph.D., and with the help of Lena Wohlschlager, M.Sc. .

## **ACKNOWLEDGMENT**

I would like to thank the associate professor Roland Ludwig for giving me the opportunity to become a member of his lab team. It was a pleasure to work and learn from all lab members. Especially, I want to thank M.Sc. Lena Wohlschlager for her patience and for great knowledge and experience she shared with me.

Zahvaljujem se i profesoru Reziću na korisnim savjetima i mentorstvu na matičnom fakultetu u Zagrebu.

Željela bih se zahvaliti prijateljima na podršci i razumijevanju koje su mi pružali sve ove godine te učinili ove studentske dane posebnima.

Na posljetku, veliko hvala mojim roditeljima i sestri koji su mi od malih nogu isticali važnost obrazovanja te bili uz mene i poticali me, kako u lijepim tako i u teškim trenutcima. Bez vas ovo ništa nebi bilo moguće!

## BASIC DOCUMENTATION CARD

Graduate Thesis

University of Zagreb  
Faculty of Food Technology and Biotechnology  
Department of Biochemical Engineering  
Laboratory for Biochemical Engineering, Industrial Microbiology and Melting and Brewing Technology

**Scientific area:** Biotechnical Sciences

**Scientific field:** Biotechnology

### PRODUCTION AND PURIFICATION OF FUNGAL ENZYMES

*Matea Zrilić, 1153/BPI*

**Abstract:** Glyoxal oxidase (GLOX) is an extracellular H<sub>2</sub>O<sub>2</sub>-generating metalloenzyme produced by various wood-degrading fungi, one of them being *Phanerochaete chrysosporium*, a white-rot fungus with the ability to completely degrade lignin. In this thesis, fermentation of *P. chrysosporium* was conducted on cellulose and sawdust from poplar as carbon sources as well as partial characterization of heterologously produced GLOX was performed. The highest activity of the enzyme was reached at pH 6.0 and the amount of copper present in the enzyme was determined using an assay setup based on complex formation with Zincon, where only 52-66% of the enzymes were found to contain a copper ion in their active site. A broad substrate screening with over 15 compounds was carried out and the highest activity was reached for the extracellular metabolite methylglyoxal. Since the detailed reaction mechanism and mode of activation of GLOX is still unclear, a screening method to test potential activators was developed.

**Keywords:** glyoxal oxidase, *Phanerochaete chrysosporium*, white-rot fungi, lignin degradation

**Thesis contains:** 50 pages, 24 figures, 15 tables, 28 references

**Original in:** English

**Graduate Thesis in printed and electronic (pdf format) version is deposited in:** Library of the Faculty of Food Technology and Biotechnology, Kačićeva 23, Zagreb.

**Mentor at Faculty of Food Technology and Biotechnology:** *Ph.D. Tonči Rezić*

**Principal mentor:** *Ph.D., Roland Ludwig*

**Technical support and assistance:** *M.Sc. Lena Wohlschlager*

#### Reviewers:

1. *Ph.D. Roland Ludwig*, Associate professor, University of Natural Resources and Life Science, Vienna
2. *Ph.D. Tonči Rezić*, Full professor, University of Zagreb
3. *Ph.D. Božidar Šantek*, Full professor, University of Zagreb
4. *Ph.D. Blaženka Kos*, Full professor, University of Zagreb (substitute)

**Thesis defended:** 01. July 2020

## TEMELJNA DOKUMENTACIJSKA KARTICA

Diplomski rad

Sveučilište u Zagrebu  
Prehrambeno-biotehnološki fakultet  
Zavod za Biokemijsko inženjerstvo  
Laboratorij za biokemijsko inženjerstvo, industrijsku mikrobiologiju i tehnologiju slada i piva

Znanstveno područje: Biotehničke znanosti

Znanstveno polje: Biotehnologija

### PROIZVODNJA I PROČIŠĆAVANJE FUNGALNIH ENZIMA

*Matea Zrilić, 1153/BPI*

**Sažetak:** Glioksal oksidaza (GLOX) izvanstanični je metaloenzim koji stvara vodikov peroksid, a proizvode ga različite gljive sa sposobnošću razgradnje drveta. Jedna od njih je i *Phanerochaete chrysosporium*, gljiva bijele truleži sa sposobnošću da u potpunosti razgradi lignin. U sklopu izrade ovog rada provedena je fermentacija *P. chrysosporium* na celulozi i piljevini topole kao izvorima ugljika te je provedena i djelomična karakterizacija heterologno proizvedenog GLOX-a. Najveća aktivnost enzima postignuta je pri pH 6.0, a količina bakra prisutna u aktivnom mjestu enzima određena je uz pomoć Zincon reagensa. Izmjerena količina bakra pokazala je da samo 52-66% enzima sadrži iona bakra u aktivnom mjestu. Provedeno je i testiranje širokog spektra supstrata s preko 15 spojeva, pri čemu je najveća aktivnost postignuta sa izvanstaničnim metabolitom, metilglioksalom. Budući da detaljan mehanizam reakcije i način aktivacije GLOX-a još uvijek nije jasan, razvijena je metoda uz pomoć koje su testirani potencijalni aktivatori.

**Gljučne riječi:** glioksal oksidaza, *Phanerochaeta chrysosporium*, gljive bijele truleži, razgradnja lignina

**Rad sadrži:** 50 stranica, 24 slike, 15 tablica, 28 literaturni navoda

**Jezik izvornika:** engleski

**Rad je u tiskanom i elektroničkom (pdf format) obliku pohranjen u:** Knjižnica Prehrambeno-biotehnološkog fakulteta, Kačićeva 23, Zagreb

**Mentor na Prehrambeno-biotehnološkom fakultetu:** *prof.dr.sc. Tonči Rezić*

**Neposredni mentor:** *izv.prof.dr.sc. Roland Ludwig*

**Pomoć pri izradi:** *M.Sc. Lena Wohlschlager*

**Stručno povjerenstvo za ocjenu i obranu:**

1. Izv.prof.dr.sc. Roland Ludwig, Sveučilište za prirodne resurse i znanost o životu, Beč
2. Prof.dr.sc. Tonči Rezić, Sveučilište u Zagrebu
3. Prof.dr.sc. Božidar Šantek, Sveučilište u Zagrebu
4. Prof.dr.sc. Blaženka Kos, Sveučilište u Zagrebu (zamjena)

**Datum obrane:** 01. Srpnja 2020.

# TABLE OF CONTENTS

<b>1. INTRODUCTION.....</b>	<b>1</b>
<b>2. THEORETICAL PART .....</b>	<b>3</b>
2.1. LIGNOCELLULOSIC BIOMASSS .....	3
2.1.1. Lignocellulose.....	3
2.2.2. Cellulose .....	4
2.2.3. Hemicellulose .....	4
2.2.4. Lignin.....	4
2.2.5. Lignocellulosic degradation.....	5
2.3. WHITE-ROT FUNGI AND THEIR LIGNIN DEGRADATION SYSTEM.....	7
2.4. GLYOXAL OXIDASE .....	7
<b>3. MATERIALS AND METHODS.....</b>	<b>11</b>
3.1. CHEMICALS, SOLUTIONS AND MEDIA .....	11
3.1.1. Chemicals.....	11
3.1.2. Buffers.....	11
3.1.3. Solutions and media.....	12
3.1.4. Enzymes .....	14
3.2. FERMENTATION AND PROTEIN PURIFICATION .....	14
3.2.1. Fermentation .....	14
3.2.2. Purification.....	16
3.3. PROTEIN CHARACTERIZATION .....	17
3.3.1. Protein concentration .....	17
3.3.2. Copper loading.....	18
3.3.4. Enzymatic assays .....	20
3.3.5. ABTS radical and phenoxy radicals generation.....	23
3.3.6. Quinones .....	24
<b>4. RESULTS AND DISCUSSION.....</b>	<b>25</b>
4.1. FERMENTATION OF <i>Phanerochaete chrysosporium</i> AND PROTEIN PURIFICATION .....	25
4.2. GLOX CHARACTERIZATION.....	28
<b>4.2.1. ABTS assay and activation.....</b>	<b>28</b>
4.2.2. Buffer testing .....	30
4.2.3. pH profile .....	31
4.2.4. Copper loading - Zincon assay .....	33



4.2.5. rGLOX reconstitution with Cu <sup>2+</sup> .....	34
4.2.6. Substrate screening .....	35
4.3. ACTIVATOR ASSAY ESTABLISHMENT .....	36
4.3.1. TMB assay .....	36
4.3.2. Amplex red assay .....	39
4.3.3. 2,6-DMP assay .....	40
4.4. rGLOX ACTIVATION .....	41
4.4.1. Quinones .....	41
4.4.2. Phenoxy radicals .....	42
<b>5. CONCLUSIONS.....</b>	<b>45</b>
<b>6. REFERENCES .....</b>	<b>47</b>

# 1. INTRODUCTION

The intensive use of fossil fuels as a source of energy, but also as a raw material for non-energy purposes, began during the first industrial revolution in the 18<sup>th</sup> century. Since then, due to the industrialization and massive population growth, the need for fossil fuels increased and resulted in depletion of available resources. Due to the lengthy process of their formation (up to several million years), it is not possible to create new sources in the near future. It is estimated that the current consumption could completely exhaust the resources in less than a century. To prevent this and eliminate the dependence on fossil fuels, science and industries need to turn to renewable energy sources, sources that are more sustainable (Henrich et al., 2015).

Lignocellulosic biomass is a widespread feedstock that, due to the low price and its favorable composition of 60-80% polysaccharides (cellulose and hemicellulose) and 15-30% of lignin, is considered as a good renewable energy source. Due to the solid and compact structure of polysaccharide and lignin network, decomposition of lignocellulosic materials, specifically the efficient separation of lignin and polysaccharides, is presenting a technological challenge and because of the complexity of the structure, pre-treatment is necessary (Den et al., 2018; Henrich et al., 2015).

Pre-treatment can be carried out using physical, chemical or biological methods. For a long time, for the sake of simple application and because they have proven successful in the breakdown of cellulose and hemicellulose, mostly physical and chemical methods were used. But, due to the harsh conditions needed in these processes, these days most industries and scientists are increasingly turning to biological methods. Also, chemical and physical methods only lead to the extraction of lignin (delignification) as a by-product with no industrial value, while the biological methods are based on the use of fungi possessing the ability to almost completely decompose lignocellulosic material, including lignin (Janušić et al., 2008).

This thesis was done as a part of the ERC-COG OXIDISE project (project number 726396) with the aim to resolve authentic conversion rates of fungal lignocellulose degrading oxidoreductases in the vicinity of/or bound onto their polymeric substrates and to elucidate their distribution and interaction. Because fungi classified as white-rots and soft-rots have a substantial arsenal of oxidoreductases dedicated to lignocellulose degradation, *Phanerochaete chrysosporium*, widely studied white-rot fungus from the Basidiomycota phylum, has been used as the model organism in this project (Riley et al., 2014).

In the lignin degradation process, two main groups of *P.chrysosporium* enzymes are involved: lignin-modifying enzymes (LME) and lignin-degrading auxiliary enzymes (LDA). LME group contains various types of enzymes, such as lignin and manganese peroxidase, that are responsible for the catalization of lignin breakdown, but for their activity H<sub>2</sub>O<sub>2</sub> is crucial. This H<sub>2</sub>O<sub>2</sub> is produced by the LDA enzymes which are unable to degrade lignin on their own yet are necessary to complete the degradation process. One of the LDA enzymes is glyoxal oxidase (GLOX), a partially investigated extracellular enzyme with a great biotechnological potential, which is why its characterization was one of the main tasks in this thesis (Daou and Faulds, 2017).

## 2. THEORETICAL PART

### 2.1. LIGNOCELLULOSIC BIOMASS

#### 2.1.1. Lignocellulose

Lignocellulosic biomass generally comprises three different types of biopolymers, namely cellulose, hemicellulose and lignin (Figure 1). The precise amount of different polymers in specific plants depends on the plant or wood species (softwood or hardwood) but usually varies between 40-50 % for cellulose, 25-35% for hemicellulose and 15-20 % for lignin (Alonso et al., 2010). Lignocellulose is the most abundant biopolymer in nature and, as a sustainable feedstock that can replace fossil fuels for energy production, it has received considerable attention in the last couple of years.

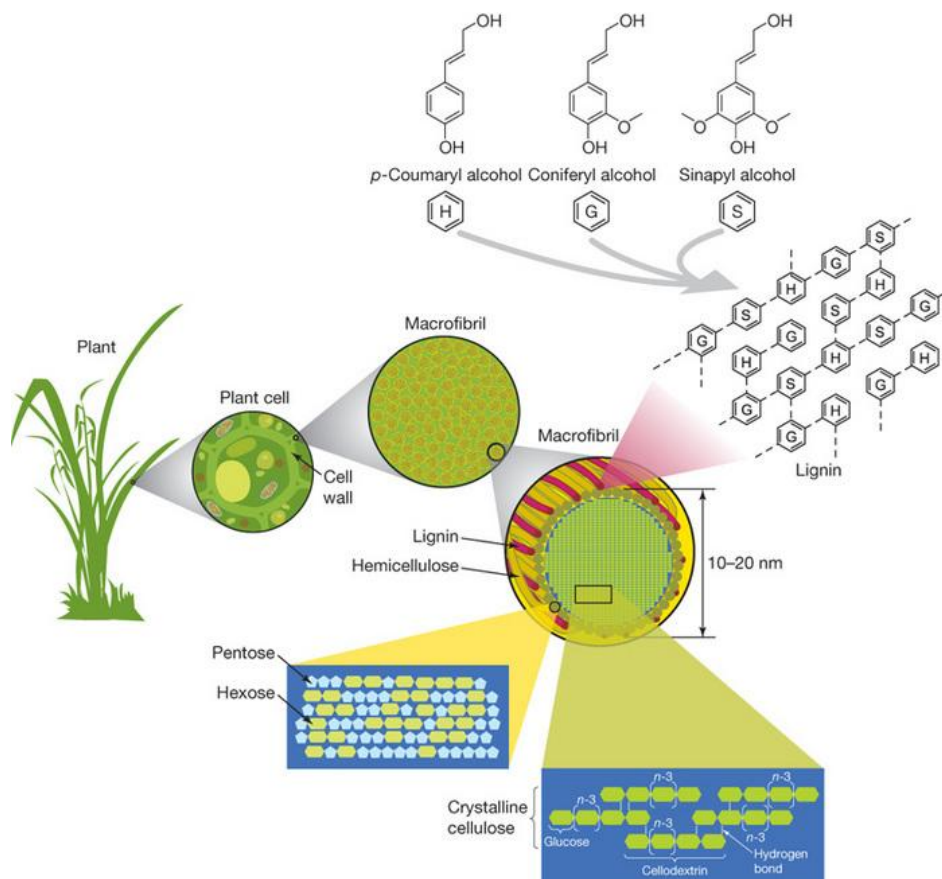


Figure 1. Structure of lignocellulose (Rubin, 2008)

### 2.2.2. Cellulose

As the main substance in the walls of plant cells, cellulose is the most common organic compound on Earth. It is a linear organic polysaccharide comprised of many glucose monosaccharides linked to one another by  $\beta(1\rightarrow4)$ glycosidic bonds. To develop carbohydrate potential, cellulose content needs to be converted into simple sugars, such as glucose and because of the cellulose structure simplicity, this conversion can easily be done by acid or enzyme catalyzation (Van Wyk, 2011).

### 2.2.3. Hemicellulose

Hemicellulose is a collective name for non-cellulose polysaccharides that show large variation, within one plant species and its tissues and between plants. It is a heteropolymer with varying degrees of branching, whose biopolymers bind bundles of cellulose fibrils to form microfibrils, which enhance the stability of the cell wall (Figure 1). They also cross-link with lignin, creating a complex web of bonds that provide structural strength. In general, enzymatically it is easier to degrade hemicellulose than cellulose, but certain oligomeric structures are recalcitrant and hard to break because of complex branching and acetylation patterns. Decomposition of hemicellulose results in a mixture of different types of sugars, including pentoses that are difficult to ferment (Horn et al., 2012; Van Wyk, 2011).

### 2.2.4. Lignin

Lignin is a relatively hydrophobic and aromatic heteropolymer consisting mainly of three different phenylpropanoid units, guaiacyl, syringyl and p-hydroxyphenyl. In the lignocellulosic biomass, lignin is crosslinked with carbohydrates by ether or ester linkages and his main function in plant wall is to give structural support, impermeability and microbial attack and oxidative stress resistance. So far, there is no simple industrial process for lignin degradation. Usually, it is expensive degradation done by co-factor-dependent oxidoreductases (Horn et al., 2012).

### 2.2.5. Lignocellulosic degradation

Due to the increasing needs and decreasing availability of fossil fuel resources, it is estimated that available supplies will be consumed in less than a century. As the generation of fossil fuels is a long process and their combustion releases large amounts of carbon dioxide, dramatically increasing global warming, a complementary strategy focused on renewable resources has been created. Therefore, lignocellulosic materials like wood, grass or straw will become a major source of raw materials and biorefineries will deconstruct complex biomass constituents into valuable raw-materials (Esposito and Antonietti, 2015).

As the only renewable carbon source for the production of all carbon products, organic bulk and fine chemicals and hydrocarbon fuels, lignocellulose is a highly valuable feedstock (Henrich et al., 2015). But, due to the compact structure and interwoven network of its constituents, degradation of lignocellulosic materials is difficult. Lignin is a complex heteropolymer of phenolic subunits that are interconnected by a variety of different bond types, the most common being  $\beta$ -O-4' aryl glycerol ether bond (~ 45%) and  $\beta$ -5-phenyl coumaran bond (~ 10%). Due to the many nonspecific bond types in the composition of lignin and its intertwining with cellulose and hemicellulose, lignin provides the plant with strength, but it is also the largest barrier to the efficient decomposition and use of lignocellulosic materials. Because of the structural complexity, in order to open up the carbohydrates compounds and make them available for microbial and/or enzymatic attacks, it is necessary to pre-treat lignocellulosic materials (Andlar et al., 2018; Den et al., 2018).

Current processes for lignocellulose deconstruction are based on thermal pretreatment and hydrolysis based on acid, base or solvents followed by enzymatic processing in some cases.

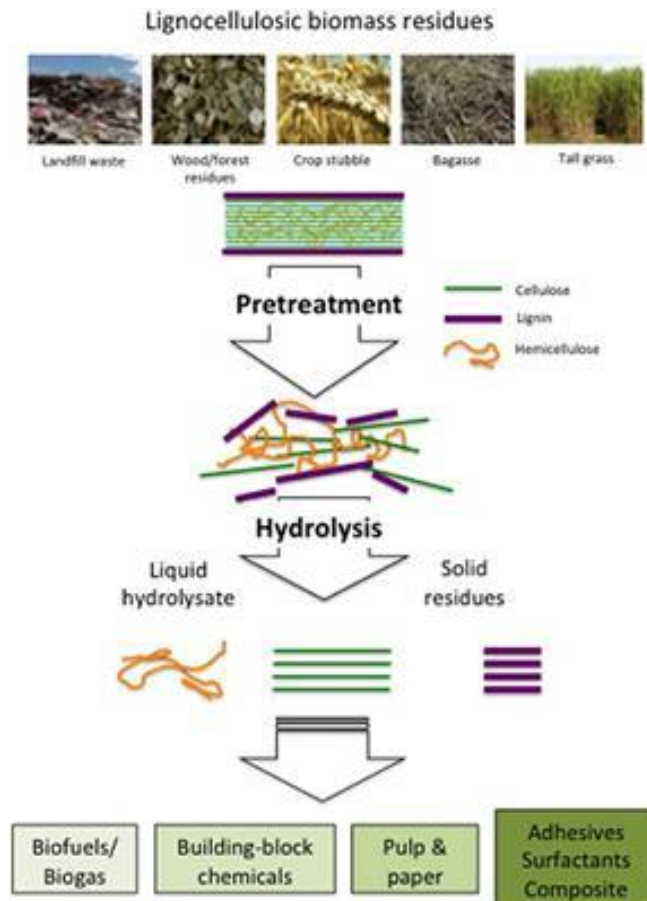


Figure 2. Conversion process of lignocellulosic biomass (Den et al., 2018)

The main problem with the most commonly used physical (mechanical comminution, steam explosion, extrusion and radiation) and chemical methods (acids, bases and solvents) of pretreatment is that lignin remains as a by-product without industrial value, which causes large losses, but also these methods are usually economically unprofitable and during the process, inhibitory compounds can be formed. In addition with chemical methods another very important problem arises and that is aggressiveness and toxicity of used chemicals and their adequate disposal after use (Kovačić 2007).

Plant cell wall-degrading filamentous fungi from the phylum of Basidiomycota and Ascomycota, have an important role in recycling nutrients in the forest ecosystem. These are wood-degradation fungi possessing two types of lignocellulose degradation systems, intracellular and extracellular. In the extracellular system, two categories of enzymes are distinguished, hydrolytic for the degradation of the polysaccharides and oxidative for the degradation of lignin and the opening of phenolic rings. In terms of effect and degradation mechanism, 3 groups of fungi are distinguished: soft-rot, brown-rot and white-rot. All these

types of fungi are able to decompose lignin, but only white-rot degrade it completely to CO<sub>2</sub> and H<sub>2</sub>O, thereby the details of the lignin degradation mechanism have been elucidated in the white rot fungus species *Phanerochaete chrysosporium* (Andlar et al., 2018; Janusz et al., 2017).

### 2.3. WHITE-ROT FUNGI AND THEIR LIGNIN DEGRADATION SYSTEM

*Phanerochaete chrysosporium* is a white-rot fungi from the Basidiomycota phylum. It is a crust fungi which forms flat fused reproductive fruiting bodies instead of the mushroom structure with a high optimum temperature of 40°C. *P.chrysosporium* is the organism most extensively studied for its lignin-degrading ability. It has the ability to break down both hardwood and softwood.

Enzymes from white-rot fungi involved in lignin breakdown can generally be divided into 2 main groups: lignin-modifying enzymes (LME) and lignin-degrading auxiliary (LDA) enzymes. LME enzymes are produced as a products of secondary metabolism, since lignin degradation does not provide any energy to the fungus. They are classified as phenol oxidase (laccases) and heme containing peroxidases (POD), namely lignin (LiP), manganese (MnP) and versatile peroxidases (VP). LDA enzymes are unable to degrade lignin on their own, but still are necessary to complete the degradation process. Some of LDA enzymes are glyoxal oxidase (GLOX), aryl alcohol oxidase (AAO), glucose dehydrogenase (GDH), pyranose 2-oxidase (POX) and cellobiose dehydrogenase (CDH) (Janusz et al., 2017).

However, the recent expansion in genome analyses has shown that the repertoire of genes varies substantially among white rot fungi, which is why for e.g *P. chrysosporium* lacks genes encoding laccases, GDH and AAO.

### 2.4. GLYOXAL OXIDASE

GLOX is an extracellular enzyme found in white-rot fungi. The best-characterized one is from *Phanerochaete chrysosporium* with the molecular mass of 68 kDA. As an LDA enzyme, GLOX is not capable of digesting lignin by itself, but essential for the degradation process. Namely, in order for peroxidases (LME enzymes) to break down lignin, they need H<sub>2</sub>O<sub>2</sub> for their catalytic activity. That H<sub>2</sub>O<sub>2</sub> is produced by GLOX, an redox-active enzyme



that uses oxygen as an electron acceptor to catalyze the reaction of simple aldehydes and  $\alpha$ -hydroxy-carbonyls (Figure 3):



Figure 3. Reaction catalyzed by GLOX (Daou and Faulds, 2017)

Attempts to resolve the crystal structure have not been successful so far, but spectroscopic studies revealed a remarkable degree of similarity in terms of active site structure and chemistry, between glyoxal oxidase and galactose oxidase (GAO) (Whittaker et al., 1996). Sequence alignment and homology modeling facilitated the identification of the catalytic residues in GLOX (Figure 4) (Daou and Faulds, 2017).

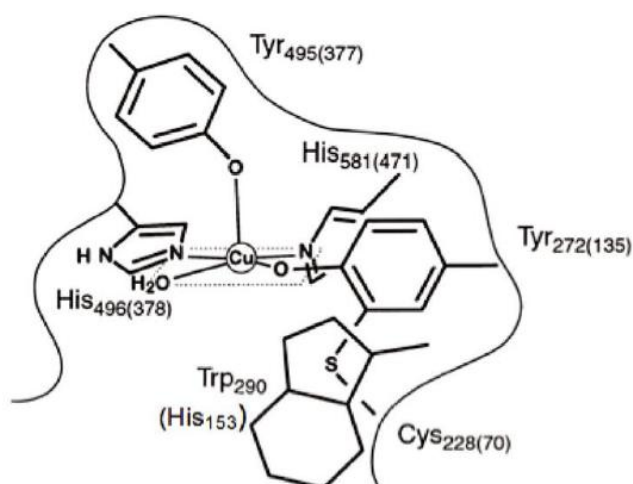


Figure 4. Active site of GLOX adapted from GAO active site (Daou and Faulds, 2017)

GLOX is a metalloenzyme that, like GAO, combines two distinct one-electron acceptors into a metalloradical complex in its active site. One is a copper metal center while the second is an unusual free radical site at a tyrosine residue that is covalently linked to a cysteine (Cys-Tyr 272) (Whittaker 2003). By transferring one electron to an activator, GLOX is oxidized and catalyzes the oxidation of a number of aldehyde and  $\alpha$ -hydroxy carbonyl compounds. Reduced GLOX, in order to regenerate itself, reduces dioxygen to hydrogen peroxide, which is the co-substrate of peroxidases.

From previous studies it has been shown that purified GLOX in its resting state is catalytically inactive, but can be reactivated by a peroxidase system. Kersten (Kersten, 1990) was the first one who conducted a series of reactions to find out what it takes to achieve full enzyme activity. He proved that GLOX can be activated by a system containing a peroxidase (e.g. lignin peroxidase) together with its substrate (e.g. veratryl alcohol). But these two enzymes and their substrates were not sufficient for immediate activation of the GLOX. Namely, during this reaction, the presence of a lag phase was observed, which was later successfully overcome by the addition of catalytic amounts of  $H_2O_2$ .

Few years later, together with Kurek, Kersten investigated in more details influence of the  $H_2O_2$  and peroxidases (POD) on rGLOX activity (Kurek and Kersten, 1995). During these studies it has been shown that peroxidase substrate itself is not activating GLOX, only in a combination with peroxidase (HRP or LiP) activation happens, which indicates that oxidized substrate of peroxidase is actually activating GLOX.

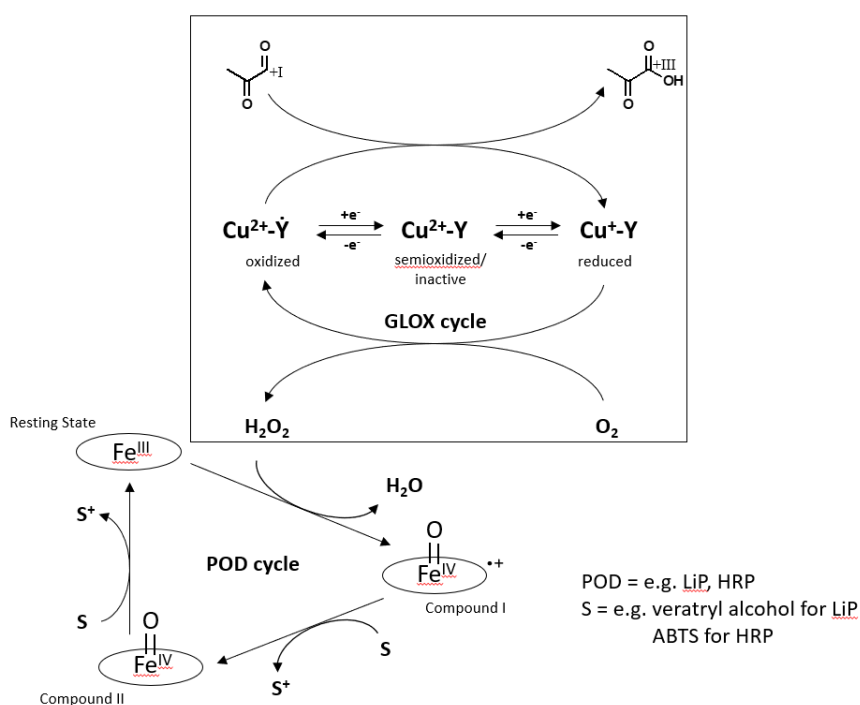


Figure 5. Proposed scheme for the catalytic mechanism of GLOX and POD

GLOX activity can be determined by measuring oxygen consumption directly with an oxygen sensor (Kersten, 1990), but also spectrophotometrically using a coupled assay to detect  $H_2O_2$  formation (Leuthner et al., 2005). However, because oxygen consumption is a time-consuming method and for higher throughput, in this thesis, a coupled assay with

horseradish peroxidase (HRP) and ABTS was used (Figure 5). ABTS can be oxidized by HRP resulting in ABTS radical, a highly colored compound that can be detected spectrophotometrically. In its catalytic cycle, HRP is oxidized by  $H_2O_2$  and subsequently reduced by oxidizing two ABTS molecules.

Because of the presence of one copper ion in its active site, GLOX is classified as radical copper oxidase (CRO), forming the AA5 family in the CAZymes system (Whittaker et al., 1996). In order to determine copper in metalloproteins, a method known as Zincon assay can be used. The method is based on the use of metal chelator Zincon, a colorimetric indicator used for spectrophotometric determination of zinc, copper and mercury. Initially, the proteins are denatured with guanidine hydrochloride whereby copper is released from the active site into solution. The released copper then binds to zincon and forms a metal-zincon complex whose formation is detected spectrophotometrically (Säbel et al., 2010).

### 3. MATERIALS AND METHODS

#### 3.1. CHEMICALS, SOLUTIONS AND MEDIA

##### 3.1.1. Chemicals

Chemicals used during this research were purchased from Sigma-Aldrich (St.Louis, Missouri, USA), Fluka (Vienna, Austria), Carl Roth (Karlsruhe, Germany) and Merck (Darmstadt, Germany) and were of analytical grade or the highest purity available.

Aqueous solutions were prepared by using water deionized with reverse osmosis (RO-H<sub>2</sub>O) or by water deionized and purified (HQ-H<sub>2</sub>O, 0.055 mS cm<sup>-1</sup>) by a Siemens Ultra clear Basic UV SG system.

##### 3.1.2. Buffers

Table 1. Buffers used in enzymatic assays

Buffer	Molarity [mM]		pH
Borate buffer	50	100	9.0
KPP buffer	50	100	6.5
MES	50	100	5.0, 6.0
Malic acid buffer	50	100	5.0, 6.0
Oxalate buffer	50	100	5.0, 6.0
Tartrate buffer	50	100	5.0, 6.0
Histidine buffer	50	100	5.0, 6.0
Acetate buffer	50	100	5.0, 6.0
Imidazole-HCl buffer	50	100	5.0, 6.0
Phosphate buffer	50	100	5.0, 6.0
MOPS	50	100	5.0, 6.5, 7.0, 7.5
Na-2,2-dimethylsuccinate buffer	50	100	3.5, 4.0, 4.5, 5.0, 5.5, 6.0, 6.5
Citrate buffer	25	50 100	3.5, 4.0, 4.5, 5.0, 5.5, 6.0, 6.5, 7.0

Table 2. Buffers for anion-exchange chromatography (AEX)

Buffer	Molarity [mM]	pH	Composition
Stock buffer	1000	7.0	57,19 g > 99,5% HEPES
Buffer A	20	7.0	1 M stock buffer
Buffer B	20	7.0	1 M stock buffer + 1M NaCl

### 3.1.3. Solutions and media

Table 3. Media for *Phanerochaete chrysosporium*

<b>Component</b>	<b>Concentration [g L<sup>-1</sup>]</b>
MCC	30
saw dust	0.5
peptone	20
NH <sub>4</sub> NO <sub>3</sub>	2.5
MgSO <sub>4</sub> · 7 H <sub>2</sub> O	1.5
KH <sub>2</sub> PO <sub>4</sub>	1.2
KCl	0.6
Streptomycin	0.05
Chlorophenikol	0.035
<b>Component</b>	<b>Concentration [mL L<sup>-1</sup>]</b>
trace metal solution	0.3

Table 4. Trace metal solution

<b>Component</b>	<b>Concentration [g L<sup>-1</sup>]</b>
ZnSO <sub>4</sub> · 7 H <sub>2</sub> O	1
MnCl <sub>2</sub> · 4 H <sub>2</sub> O	0.3
H <sub>3</sub> BO <sub>3</sub>	3
CoCl <sub>2</sub> · 6 H <sub>2</sub> O	2
CuSO <sub>4</sub> · 5 H <sub>2</sub> O	0.1
NiCl <sub>2</sub> · 6 H <sub>2</sub> O	0.2
H <sub>2</sub> SO <sub>4</sub>	4

Table 5. Assay solutions

<b>Solution</b>	<b>Molarity [mM]</b>	<b>Solvent</b>
ABTS	10	HQ-H <sub>2</sub> O
Methyl glyoxal	1000	HQ-H <sub>2</sub> O
Guanidine hydrochloride	4710	50 mM borate buffer pH 9.0
Zincon solution	0.8	HQ-H <sub>2</sub> O
DCIP solution	3	10% EtOH
Lactose solution	300	HQ-H <sub>2</sub> O
Syringol solution	10	HQ-H <sub>2</sub> O
MnSO <sub>4</sub> solution	5	HQ-H <sub>2</sub> O
H <sub>2</sub> O <sub>2</sub> solution	0.5	HQ-H <sub>2</sub> O
Veratryl alcohol	10	HQ-H <sub>2</sub> O
Amplex red solution	10	DMSO
TMB	50	DMSO

Table 6. Substrate solutions

<b>Solution</b>	<b>Molarity [mM]</b>	<b>Solvent</b>
Methyl glyoxal	1000	HQ-H <sub>2</sub> O
2,3-Butanediol	1000	HQ-H <sub>2</sub> O
Glyoxal	100	HQ-H <sub>2</sub> O
D-(+)-Glyceraldehyde	100	96% EtOH
L-(+)-Glyceraldehyde	100	96% EtOH
Acetaldehyde	1000	HQ-H <sub>2</sub> O
Formaldehyde	1000	HQ-H <sub>2</sub> O
Glyoxylic acid	1000	HQ-H <sub>2</sub> O
Veratryl aldehyde	100	96% EtOH
Benzyl alcohol	100	96% EtOH
D-(+)-Glucose	100	HQ-H <sub>2</sub> O
D-(+)-Cellobiose	100	HQ-H <sub>2</sub> O
D-(+)-Galactose	100	HQ-H <sub>2</sub> O
1,3-propanediol	1000	HQ-H <sub>2</sub> O
Dimethylglyoxal	1000	HQ-H <sub>2</sub> O
Formic acid	1000	HQ-H <sub>2</sub> O
Dihydroxyacetone	1000	96% EtOH
Glycerol	1000	96% EtOH

Table 7. Activator solutions

<b>Solution</b>	<b>Molarity [mM]</b>	<b>Solvent</b>
Tetrafluoro-1,4-benzoquinone	1	DMSO
Methoxy-1,4-benzoquinone	5	HQ-H <sub>2</sub> O
2,6-Dimethyl-1,4-benzoquinone	5	DMSO
2,6-Dimethoxy-1,4-benzoquinone	5	DMSO
Veratryl alcohol	10	96% EtOH
Guaiacol	10	HQ-H <sub>2</sub> O
Caffeic acid	100	96% EtOH
Ferulic acid	100	DMSO
Catechol	10	HQ-H <sub>2</sub> O
Coumeric acid	100	DMSO
Vanillic acid	100	DMSO
Syringic acid	100	DMSO
Acetosyringone	100	DMSO
Syringaldehyde	100	96% EtOH
Coniferyl alcohol	100	96% EtOH
TEMPO	100	DMSO
1-Hydroxybenzotriazole hydrate (HOBt)	100	DMSO

#### 3.1.4. Enzymes

Recombinant glyoxal oxidase (rGLOX), whose characterization was the goal of the second part of this thesis, was produced in both *Pichia pastoris* strain X33 and *Trichoderma reesei* strain QM9414  $\Delta$ xyr1. The production process, consisted of fermentation followed by a two-step purification: hydrophobic interaction chromatography (HIC) and anion exchange chromatography (AEX), resulted in enzymes with purity higher than 95% according to SDS-PAGE analysis.

Peroxidase from horseradish, which was used in the ABTS assay, was obtained from Sigma-Aldrich.

Glucose oxidase from *Aspergillus niger*, which was used to test the O<sub>2</sub> sensor, was purchased from Sigma-Aldrich.

Laccase from *Botrytis aclada*, which was used to oxidize potential activators, was produced by another lab member in *P. pastoris*.

### 3.2. FERMENTATION AND PROTEIN PURIFICATION

#### 3.2.1. Fermentation

##### 3.2.1.1. Pre-pre culture

*P.chrysosporium* ATCC 24725 strain was grown on PDA (Potato Dextrose Agar) plate. After 10 days, 5 mL of PDB (Potato Dextrose Broth) was added to scrape off the mycelium and to collect it in a Falcon tube. Three 1-L flasks, containing 200 mL PDB medium, were inoculated with 1 mL each of the mycelium suspension and covered with a steril air filter and a metal cap. The flasks were incubated at 30°C and 80 rpm for 2 h afterward the shaking speed was increased to 100 rpm for another 72 h.

##### 3.2.1.2. Pre-culture

Supernatant from the prepre-culture flasks was decanted and mycelium, together with residual medium, was homogenized using the Ultra turrax with a sterile tip. As a result, homogeneous mycelium was obtained and used for the inoculation of pre-culture flasks. The medium in the flasks was of the same composition as the fermentation medium. In total there

were six 1-L flasks containing 300 mL of medium, each inoculated with 2 mL mycelium suspension. Flasks were incubated at 30°C and 95 rpm for 48 h.

### 3.2.1.3. Fermentation

*P.chrysosporium* fermentation was conducted in a 10-L scale with microcrystalline cellulose (MCC) and saw dust from poplar as a carbon sources. Fermentation media ( Table 3) also contained  $\text{MgSO}_4 \cdot 7 \text{H}_2\text{O}$ ,  $\text{KH}_2\text{PO}_4$ , KCl and trace metal solution (Table 4). As a protein and nitrogen sources, peptone from meat and  $\text{NH}_4\text{NO}_3$  were added. In order to ensure sterile working conditions the fermenter (Figure 6) was filled with water,  $\text{NH}_4\text{NO}_3$ ,  $\text{MgSO}_4 \cdot 7 \text{H}_2\text{O}$ ,  $\text{KH}_2\text{PO}_4$  and autoclaved at 121 °C for 30 min. To prevent clogging of the air diffuser, MCC, saw dust and peptone were autoclaved separately and subsequently pumped into the fermenter in a sterile manner. Afterwards, trace metal elements, as well as the antibiotics streptomycin and chlorophenikol, were injected using a syringe and a sterile filter. The fermentation was carried out as a batch process. The inoculum volume was 1 L which is 10% of the media volume. Fermentation was run for 8 days at 30°C and at pH 5.0. To keep the pH value stable during the fermentation, NaOH (1M) and  $\text{H}_3\text{PO}_4$  (1M) were used. Cultivation was aerobic with an airflow of  $5 \text{ L min}^{-1}$  and agitation of 200 rpm.

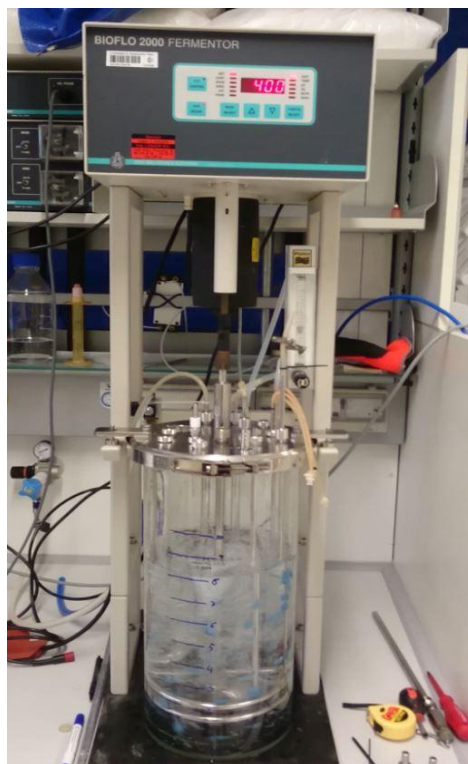


Figure 6. Fermenter



### 3.2.2. Purification

#### *3.2.2.1. Vacuum and tangential filtration*

The first step of purification was vacuum filtration used to separate the biomass from the culture liquid. Separation was performed via filter paper and to accelerate the filtration, vacuum was used.

The obtained supernatant was purified and concentrated by tangential filtration, also known as a cross-flow filtration. To perform this type of filtration, a MiniKros Plus tangential flow filtration module was used. In a first step, the hollow fiber module with a pore size of 0.22  $\mu\text{m}$  was used to remove particles and then a hollow fiber module with a molecular weight cut-off (MWCO) of 10 kDa was used to concentrate the supernatant.

#### *3.2.2.2. Anion exchange chromatography (AEX)*

The second step of the purification was an anion exchange chromatography which was performed using an ÄKTA Pure system (GE Healthcare Bio-Sciences, Pittsburgh, Pennsylvania, USA). Employed buffers and specifications of the utilized column are listed in a Table 2.. The column was flushed with buffer B and then equilibrated with buffer A. The sample was loaded onto the column (flow rate 20  $\text{mL min}^{-1}$ ) and the column was washed with buffer A to elute all unbound proteins. The elution was carried out in two gradients and fractions were collected with volumes of 250 mL.

Table 8. Column description and settings for AEX

<b>Column</b>	<i>DEAE-Sepharose Fast Flow</i>
<b>Column Volume</b>	600 mL
<b>Buffer A</b>	20 mM HEPES pH 7.0
<b>Buffer B</b>	20 mM HEPES pH 7.0 + 1M NaCl
<b>Flowrate Sample Application</b>	20 mL min <sup>-1</sup>
<b>Gradient</b>	<b>Gradient 1:</b> 0-50% buffer B in 3250 mL ( 6 column volumes) <b>Gradient 2 :</b> 50-100% buffer B in 1500 mL ( 3 column volumes)
<b>Device</b>	ÄKTA pure (GE Healthcare)

The fractions and flow-through were screened for enzyme activity as described in section 4.1. Pooled fractions were concentrated using the MiniKros Plus tangential flow filtration module and Vivaflow 50 module with a MWCO of 10 kDa (Sartorius, Gottingen, Germany) and finally centrifugal filters until a protein concentration of 10 mg mL<sup>-1</sup> was achieved.

### 3.3. PROTEIN CHARACTERIZATION

#### 3.3.1. Protein concentration

##### 3.3.1.1. Bradford protein assay

The total protein concentration in the fermentation culture was determined using the Bradford assay. The reagent and BSA standards were purchased from Bio-Rad Laboratories (Hercules, California, USA) and prepared due to the manufacturer's instructions. The assay was performed by adding 600 µL of Bradford reagent and 15 µL of diluted sample in a disposable cuvette and incubating it for 15 min at room temperature. For the measurements, a Beckman Coulter DU 800 spectrophotometer (Beckman Coulter, Brea, California, USA) was used, measuring the absorption at 595 nm. The protein concentration was calculated using a calibration curve of BSA in the range of 0.1 – 1.0 mg mL<sup>-1</sup>.

### 3.3.1.2. NanoDrop™ 2000/2000c Spectrophotometer

To determine the total protein concentration of purified enzyme samples, the absorbance at 280 nm was measured using a NanoDrop 2000/2000c spectrophotometer and the concentration was calculated according to Lambert-Beer's law. The extinction coefficient and the molecular weight of the enzyme were determined from its amino acid sequence (GenBank ID: AAA87594.1).

At first, the signal peptide was identified by the software tool "SignalP" (<http://www.cbs.dtu.dk/services/SignalP/>) and removed. The sequence lacking the signal peptide was used in another software tool "ProtParam" (<https://web.expasy.org/protparam/>) to calculate the extinction coefficient ( $35,3 \text{ mM}^{-1} \text{ cm}^{-1}$ ) and the molecular weight (57.7 kDa).

Lambert-Beer's Law:

$$A = \varepsilon \times c \times d$$

A – absorption

$\varepsilon$  – molar extinction coefficient [ $\text{M}^{-1} \text{ cm}^{-1}$ ]

c – molar concentration [M]

l – pathlength [cm]

### 3.3.2. Copper loading

The amount of GLOX being loaded with copper was determined by spectrophotometric method using the zincon assay. For the calibration curve,  $\text{CuCl}_2$  solution was measured with the concentrations given in Table 9.

Table 9. Standards concentrations

<b>Standards</b>	
<b>Stock concentration [<math>\mu\text{M}</math>]</b>	<b>Final concentration [<math>\mu\text{M}</math>]</b>
0	0
10	1
20	2
50	5
100	10
200	20
300	30
400	40

Calibration samples:

- 100  $\mu\text{L}$  stock solution  $\text{CuCl}_2$  (in HQ- $\text{H}_2\text{O}$ )
- 850  $\mu\text{L}$  4.71 M guanidine hydrochloride
- 50  $\mu\text{L}$  zincon solution

The reaction was started by the addition of the Zincon solution. Samples were incubated for 10 min at  $21^\circ\text{C}$  and the absorption was measured at 610 nm.

Before conducting the assay, to remove the storage buffer components, the enzyme samples were re-buffered to HQ- $\text{H}_2\text{O}$  in centrifugal filters.

Enzyme samples:

- 75  $\mu\text{L}$  enzyme suspension [ $2.2 \mu\text{g mL}^{-1}$ ]
- 637.5  $\mu\text{L}$  borate buffer with guanidine hydrochloride pH 9.0
- 37.5  $\mu\text{L}$  zincon solution

The reaction and measurements were carried out in the same manner as for the calibration samples. The absorbance recorded at 610 nm was compared with the calibration curve generated with copper chloride.

### 3.3.2.1. rGLOX reconstitution with $\text{Cu}^{2+}$

Reconstitution was based on enzyme incubation with  $\text{CuSO}_4$  solution in different concentrations. For the reconstitution, two different incubation conditions were tested and the incubation lasted 23 h with activity measurements conducted after 3 h and 23 h. For the activity measurements, the standard ABTS activity assay was used.

Table 10. Reconstruction conditions

Buffer	$\text{CuSO}_4$ solution [mM]	Incubation conditions [ °C]
Acetate buffer 50 mM pH 5.0	0	21
		4
MES buffer 50 mM pH 6.0	0.1	21
		4
Borate buffer 50 mM pH 9.0	1	21
		4

### 3.3.4. Enzymatic assays

Enzymatic assays were measured spectrophotometrically either using a Perkin Elmer Lambda 35 UV-Visible Spectrometer or an Agilent 8453 UV-visible spectroscopy system (diode-array). The obtained result was the positive slope (increase) of the absorption at a reagent-specific wave length. To convert the results into  $\text{U mL}^{-1}$ , the slope was multiplied with the enzyme factor (EF). One unit ( $1\text{U} = \mu\text{mol min}^{-1}$ ) is defined as the amount of the enzyme that catalyzes the conversion of one micromole of substrate per minute under the specified conditions of the assay method.

$$\mathbf{EF} = \frac{(\text{total cuvette volume} \times \text{sample dilution} \times \text{time factor})}{(\text{enzyme volume} \times \text{pathlength} \times \text{molar absorption coefficient})}$$

#### 3.3.4.1. CDH activity assay with DCIP

- 100  $\mu\text{L}$  3 mM DCIP solution
- 100  $\mu\text{L}$  300 mM lactose solution
- 760  $\mu\text{L}$  100 mM Na-acetate buffer pH 4.0
- 20  $\mu\text{L}$  sample (clear supernatant)

All solutions were pipetted into a 1 mL microcuvette except the sample and incubated at 30°C in a water bath for 20 min. The reaction was started by addition of sample and the absorption was measured at 520 nm. Absorption coefficient ( $\epsilon$ ) = 6.9 mM<sup>-1</sup>cm<sup>-1</sup>.

#### 3.3.4.2. MnP activity assay using syringol (2,6-dimethoxyphenol)

- 100  $\mu$ L 10 mM Syringol solution
- 100  $\mu$ L 5 mM MnSO<sub>4</sub> solution
- 10  $\mu$ L 10 mM H<sub>2</sub>O<sub>2</sub> solution
- 770  $\mu$ L 50 mM Na-tartrate pH 4.5
- 20  $\mu$ L sample (clear supernatant)

All solutions were pipetted into a 1 mL microcuvette except the sample and incubated at 30°C in a water bath for 20 min. The reaction was started by addition of sample and the absorption was measured at 469 nm. Absorption coefficient ( $\epsilon$ ) = 53.2 mM<sup>-1</sup>cm<sup>-1</sup>.

#### 3.3.4.3. LiP activity assay

- 100  $\mu$ L 10 mM veratryl alcohol
- 10  $\mu$ L H<sub>2</sub>O<sub>2</sub> solution
- 870  $\mu$ L 100 mM Na-tartrate pH 4.0
- 20  $\mu$ L sample (clear supernatant)

All solutions, except H<sub>2</sub>O<sub>2</sub> and the sample, were pipetted into a 1 mL microcuvette and incubated at 30°C in a water bath for 20 min. The reaction was started by addition of H<sub>2</sub>O<sub>2</sub> and sample. The absorption was measured at 310 nm. Absorption coefficient ( $\epsilon$ ) = 9.3 mM<sup>-1</sup>cm<sup>-1</sup>.

#### 3.3.4.4. ABTS activity assay

- 860  $\mu$ L 50 mM MES buffer pH 6.0
- 100  $\mu$ L ABTS/POD reagent
- 20  $\mu$ L enzyme sample
- 10  $\mu$ L 500  $\mu$ M H<sub>2</sub>O<sub>2</sub> solution

- 10  $\mu\text{L}$  1M methyl glyoxal solution

Buffer was aerated for 15 min and then added to a micro-cuvette in a water bath for 15 min at 30°C. ABTS/POD reagent was pipette in and incubated for 2 more minutes. After that, all the other solutions were added except methyl glyoxal. The reaction was started by the addition of methyl glyoxal and the absorption was measured at 420 nm. Absorption coefficient ( $\epsilon$ ) = 36  $\text{mM}^{-1}\text{cm}^{-1}$ .

#### 3.3.4.5. Amplex red activity assay

- 760  $\mu\text{L}$  50 mM MES buffer pH 6.0
- 100  $\mu\text{L}$  500  $\mu\text{M}$  AMPLEX RED solution
- 100  $\mu\text{L}$  POD (1428 U  $\text{mL}^{-1}$ )
- 10  $\mu\text{L}$  1M methyl glyoxal
- 10  $\mu\text{L}$  500  $\mu\text{M}$   $\text{H}_2\text{O}_2$  solution
- 20  $\mu\text{L}$  enzyme

Buffer was aerated for 15 min and then added into a transparent plastic cuvette in a water bath for 15 min at 30°C. POD reagent was pipette in and incubated for 2 more minutes. After that, all the other solutions were added except the enzyme. The reaction was started by the addition of enzyme and the absorption was measured at 571 nm. Absorption coefficient ( $\epsilon$ ) = 63  $\text{mM}^{-1}\text{cm}^{-1}$ .

#### 3.3.4.6. DMP activity assay

- 850  $\mu\text{L}$  50 mM MES buffer pH 6.0
- 10  $\mu\text{L}$  100mM 2,6-DMP solution
- 100  $\mu\text{L}$  POD (1428 U  $\text{mL}^{-1}$ )
- 10  $\mu\text{L}$  1M methyl glyoxal
- 10  $\mu\text{L}$  500  $\mu\text{M}$   $\text{H}_2\text{O}_2$  solution
- 20  $\mu\text{L}$  enzyme [2.2  $\mu\text{g mL}^{-1}$ ]

Buffer was aerated for 15 min and then added into a transparent plastic cuvette in a water bath for 15 min at 30°C. 2,6-DMP and POD solutions were pipetted in and incubated for 2 more minutes. After that, all the other solutions were added except the enzyme. The

reaction was started by the addition of enzyme and the absorption was measured at 469 nm. Absorption coefficient ( $\epsilon$ ) = 53.2 mM<sup>-1</sup>cm<sup>-1</sup>.

#### 3.3.4.7. TMB activity assay :

- 858  $\mu$ L 50 mM Na-2,2-DMS buffer pH 6.0
- 100  $\mu$ L POD reagent
- 2  $\mu$ L 50 mM TMB solution
- 10  $\mu$ L 1M methyl glyoxal solution
- 20  $\mu$ L enzyme [2.2  $\mu$ g mL<sup>-1</sup>]

Buffer was aerated for 15 min and then added into a transparent plastic cuvette in a water bath for 15 min at 30°C. POD reagent was pipette in and incubated for 2 more minutes. After that, all other solutions were added except the enzyme. The reaction was started by the addition of enzyme and the absorption was measured at 650 nm. Absorption coefficient ( $\epsilon$ ) = 59 mM<sup>-1</sup>cm<sup>-1</sup>.

#### 3.3.5. ABTS radical and phenoxy radicals generation

ABTS radical and all phenoxy radicals were created using *laccase* from *Botrytis aclada*. Five milliliters of 1 mM ABTS/phenoxy radical solution was prepared in 25 mM citrate buffer pH 4.0 and converted by using 8.653 U of laccase. ABTS/phenoxy radical solution in the presence of laccase was incubated for 3min at 30°C and then centrifuged for 10 min (4000 rpm, 4°C) in an Amicon centrifugal filter with a MWCO of 10 kDa for the purpose of laccase removal. Oxidation success was detected spectrophotometrically using the NanoDrop 2000/2000c Spectrophotometer. Filtrate, ABTS radical solution, was aliquoted, frozen at -80°C and stored at -20 °C, while phenoxy radicals solutions were used directly in an enzymatic assay.



### 3.3.6. Quinones

All reactions were carried out in 50 mM MES buffer pH 6.0 and at 30°C. Quinone solutions from (Table 7) were further diluted to stocks of 0.5 mM in HQ-H<sub>2</sub>O to minimize the final concentration of DMSO in the cuvette. The final concentration of quinones was 5 μM and the samples were measured in triplicates.

## 4. RESULTS AND DISCUSSION

Two major objectives are targeted in this thesis. The first goal was to conduct the fermentation of the native fungus, *P.chrysosporium*, and to isolate the extracellular enzymes, including GLOX, from the culture. The second part of the thesis was based on the investigation of the physiochemical properties of recombinant GLOX (rGLOX) which was produced by expression from *P.pastoris* and *T.reesei*.

### 4.1. FERMENTATION OF *Phanerochaete chrysosporium* AND PROTEIN PURIFICATION

Pre-pre culture cultivation was performed on a PDA plate with daily growth monitoring. After 10 days, it was observed that the mycelium had nicely overgrown the plate, causing the end of further cultivation. Grown mycelium was used for the inoculation of liquid pre-cultures, where after three days formation of nicely shaped pellets has been observed (Figure 7). The pellets were homogenized and used for pre-culture medium inoculation. Cultivation ended after two days with the formation of mycelium agglomerates (Figure 8). The flasks were observed under the microscope for bacterial contamination. Three flasks without contamination and with nicely grown mycelium were chosen for the fermentor inoculation.

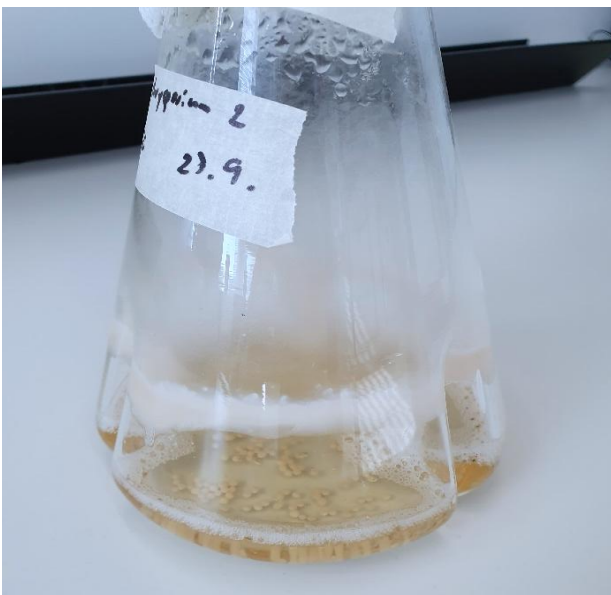


Figure 7. Pre-pre culture



Figure 8. Pre-culture

Cultivation of native *P.chrysosporium* was performed on MCC and sawdust in a volume of 10 L. The fermentation lasted for 8 days and was monitored daily. Hydrolytic activity in the medium was measured every other day by a colleague. After 8 days, due to the excessive amount of produced biomass, the uniform transport of oxygen and nutrients throughout the medium was no longer possible, resulting in the decision to stop the fermentation. Harvesting was carried out by filtration through filter paper using a vacuum pump and a Büchner funnel. Because of the interest in extracellular enzymes, the filtrate was used in further purification and analysis processes, while the remaining biomass was autoclaved and disposed properly.

After vacuum and tangential filtration, the remaining filtrate was purified performing anion exchange chromatography with a DEAE column (Figure 9).

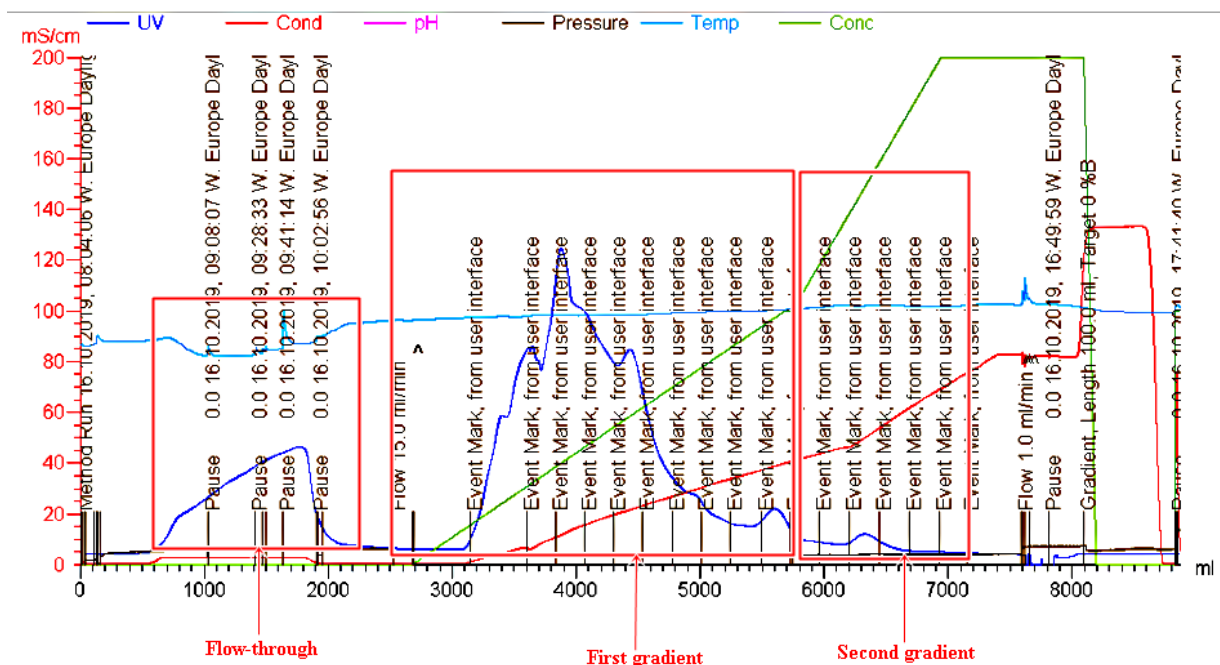


Figure 9. AEX chromatogram

Elution was conducted in two gradients resulting in 19 fractions all together. The volume of each fraction was 250 mL. The first peak represents the flow-through, all components that were not bound to the column. To check if any of desired proteins did not bind to the column these fractions were analyzed together with selected fractions of both elution gradients. Fractions marked in Figure 10 were analyzed and checked for protein concentration and enzyme activity.

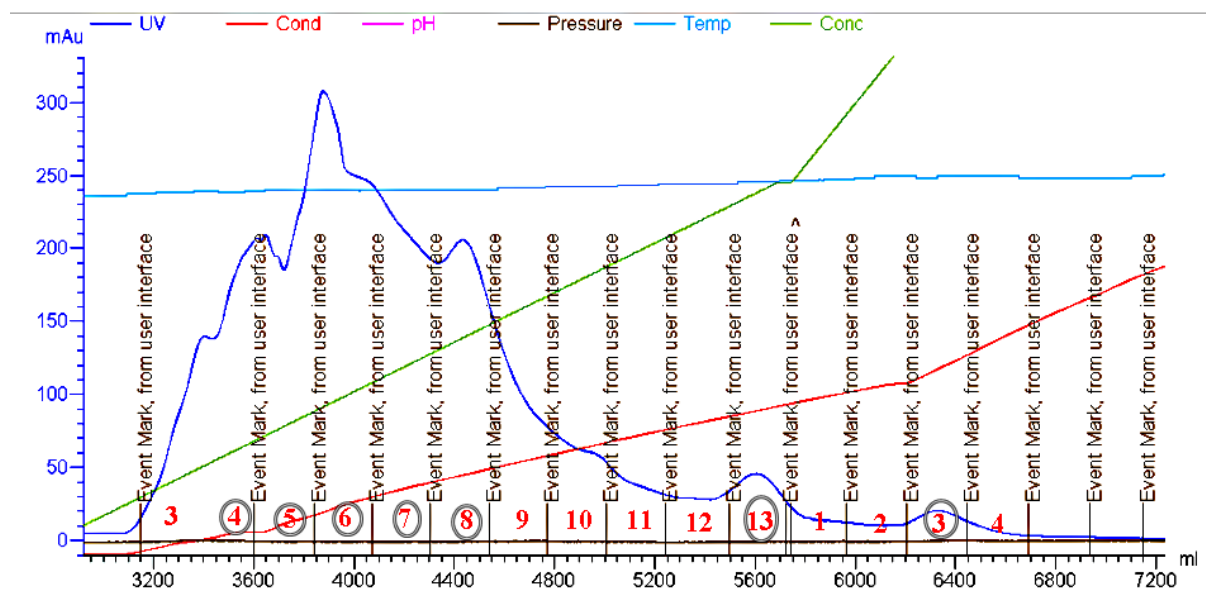


Figure 10. Selected peaks eluted in first and second gradient

The indicated fractions (Figure 10) were screened for the presence of several oxidoreductases, namely for cellobiose dehydrogenase using the DCIP assay, manganese peroxidase using syringol, lignin peroxidase using veratryl alcohol and GLOX using the coupled ABTS/HRP assay. Unfortunately, all assays were completed with negative results, which means that there was no activity of the required enzymes. Since the type and amount of enzymes expressed by fungi depend on the carbon source type and amount of present oxygen, what could be done differently is the usage of different carbon sources. For e.g. instead of MCC, pure glucose or xylose could be used, which proved to be successful in other publications (Kersten, 1990).

Despite the presence of oxidoreductases, the presence of hydrolases was also checked and detected by the colleague in the flow-through and all the fractions (Table 11). Since the main goal of this experiment was production and isolation of oxidoreductases but lack of detectable activities thereof, no further purification was carried out, as the separation of hydrolases was not the desired target at that time. Gradient fractions were pooled together and as well as flow-through, concentrated to  $10 \text{ mg mL}^{-1}$  and stored at  $-80^\circ\text{C}$  as a hydrolysis cocktail of *P. chrysosporium*.

Table 11. Hydrolysis activity and protein concentration

Fraction	Enzymatic activity		Protein concentration
	U mL <sup>-1</sup>	U mg <sup>-1</sup>	mg mL <sup>-1</sup>
4	1.49	18.21	0.08
5	0.73	4.88	0.15
6	1.48	5.23	0.28
7	0.90	6.09	0.15
8	0.50	2.94	0.17
13	0.40	21.93	0.02
3	0.37	44.63	0.01
Flow-through	1.59	33.50	0.05

## 4.2. GLOX CHARACTERIZATION

### 4.2.1. ABTS assay and activation

When it comes to GLOX reactivation, in previous studies Kurek and Kersten (Kurek and Kersten, 1995) tested the effect of lignin peroxidase and horseradish peroxidase on rGLOX activity. The tests were performed with several different peroxidase substrates which resulted in multiple and divergent effects on rGLOX activity. This led to the conclusion that peroxidase itself has no effect on rGLOX, but that the oxidized peroxidase product actually can act as an activator.

Throughout this thesis, as the main assay for rGLOX activity, an ABTS assay (3.3.4.4. ABTS activity assay) together with HRP was used. Relying on the previously mentioned conclusions of Kurek and Kersten (Kurek and Kersten, 1995) that the oxidation product is actually activating rGLOX, the influence of HRP-oxidized product, ABTS radical, was tested.

In order to determine the ABTS radical activation power, an adjusted ABTS activity assay was performed whereby the ABTS radical was used in exchange for H<sub>2</sub>O<sub>2</sub>. The results (Figure 11) shows that the ABTS radical in a final concentration of 5 μM (blue line) has the same effect on rGLOX activation as the addition of 5 μM of H<sub>2</sub>O<sub>2</sub> (red line), essential to overcome the lag phase present in a sample where no additional H<sub>2</sub>O<sub>2</sub> was added (Figure 11). The added amount of H<sub>2</sub>O<sub>2</sub> is not activating GLOX, but is immediately used by HRP which subsequently oxidizes the ABTS molecules to the ABTS radicals which then activates

rGLOX. Also, that is the reason why the measured absorbance of the samples with H<sub>2</sub>O<sub>2</sub> and ABTS radical start at a higher initial absorbance than the sample without activator. What is significant is the lag phase in the first 200 s of measurement time when there is no activator present and the equal slope of the curves when maximum activity was reached after full activation (either by the addition of the activator, ABTS radical, or by in situ generation of ABTS radical over the course of the assay)(Figure 11).

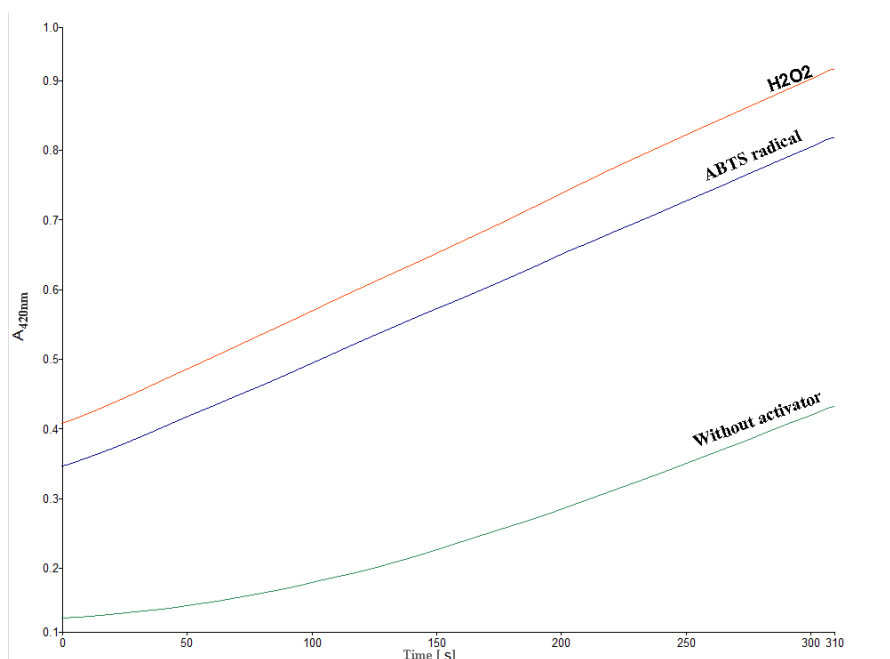


Figure 11. GLOX activity in the presence and absence of H<sub>2</sub>O<sub>2</sub> and ABTS

During the study of the ABTS radical activation potential, a great instability of the ABTS radical was detected. Instability occurred depending of the buffer composition and due to the strong illumination. According to the previously published data, ABTS radical instability appears in "Good buffers", for example MES or TES, that catalyze the reduction of the colored ABTS radical cation back to the reduced form causing a reduction of the absorbance at 420 nm (McCoy-Messer JM and Bateman RC Jr. 1993).

These results were verified and confirmed in MES and MOPS buffers during which the light sensitivity of the ABTS radical was detected. Namely, while performing the assays in spectrophotometers it was observed that frequent shooting and the use of strong UV-light, causes radical instability, which is why it is advisable to use only the VIS light that is necessary for the measurement and to record it at slightly longer intervals (approximately every 3-5 seconds).

#### 4.2.2. Buffer testing

In order to see if certain buffer will affect the enzyme and to determine in which buffer composition enzyme activity will be the highest, 11 different buffers shown in Table 12., were tested at two different pH values, pH 5.0 and pH 6.0. All buffers were of the same molarity (100 mM) and to determine enzymatic activity the ABTS activity assay was used (3.4.3. Enzymatic assays).

Table 12. List of buffers used for testing

Species (100 mM)	pH	
	5.0	6.0
Oxalic acid		X
Acetic acid	X	X
2.2-dimethyl succinic acid	X	X
Tartaric acid	X	X
Malic acid	X	X
Citrate	X	X
Imidazole-HCl	X	X
Phosphate	X	X
Histidine	X	X
MES	X	X
MOPS		X

X – used buffer

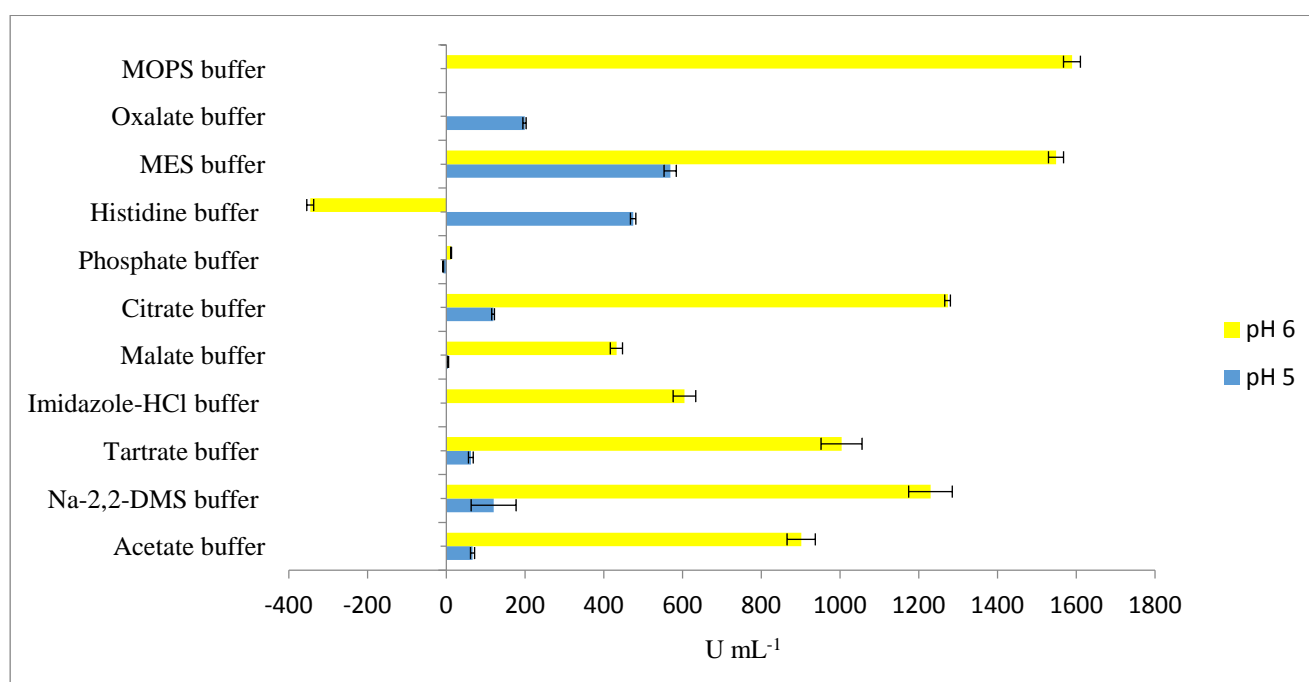


Figure 12. Enzymatic activity in selected buffers at two different pH values

From the obtained result, it is clearly visible that rGLOX is more active at pH 6.0 than pH 5.0. The highest enzyme activity was detected in MOPS buffer at pH 6.0, followed by a MES buffer, citrate buffer and sodium-2,2-dimethyl succinate buffer at the same pH value.

Inhibitory effect of phosphate buffer (pH 5.0 and pH 6.0) on enzyme activity (Figure 12), also has been observed before by Whittaker (Whittaker et al., 1996) and could be caused by spherical phosphate effects, such as blocking the substrate access to the active site (Whittaker et al., 1995). What appears to be a negative activity in histidine buffer at pH 6.0, could potentially be a consequence of the instability of ABTS radical, because as the  $H_2O_2$  is always added to the assay cuvette to overcome the lag phase, a certain amount of ABTS radical is formed before reaction with GLOX is initiated. When there is no reaction with GLOX, but the ABTS radical is reduced back by e.g. interaction with a buffer species or a substrate, this is observed as a decrease in the absorbance at 420 nm, falsely indicating a negative activity. But in order to be sure and to explain these results in more details, further investigations need to be made and a better understanding of the enzymes active site is required.

#### 4.2.3. pH profile

After testing and detection of the buffer with the best effect on enzyme activity (Figure 12) was done, a pH profile for rGLOX was measured ranging from pH 3.5 to pH 7.5 in increments of 0.5 pH units. In order to get the most reliable results, the use of "Good buffers" was avoided as far as possible, which is why MES buffer was not used. Table 13. shows certain buffers that were ultimately used to measure the pH profiles. Among these buffers, it can be seen that despite the aforementioned shortcomings, a "Good buffer", namely MOPS, was still used. The reason is that among the previously tested buffers only MOPS and phosphate buffer were able to go higher than pH 7.0 and ABTS radical instability in "Good buffers" had a significantly smaller effect on enzyme activity than the inhibitory effect of phosphate buffer (Whittaker et al., 1996).



Table 13. Buffers used for pH profile

Buffer (100 mM)	pH values
Na-2,2-dimethylsuccinate buffer	3.5, 4.0, 4.5, 5.0, 5.5, 6.0, 6.5
Citrate buffer	3.5, 4.0, 4.5, 5.0, 5.5, 6.0, 6.5, 7.0
MOPS buffer	6.5, 7.0, 7.5

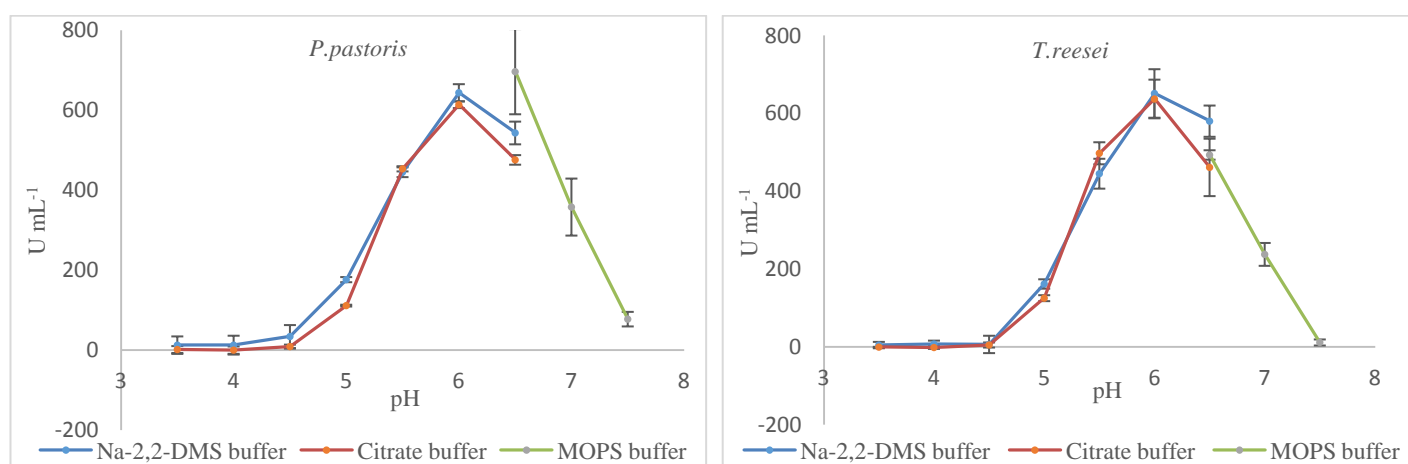


Figure 13. GLOX pH profiles in *P. pastoris* and *T. reesei*

The pH profiles (Figure 13) were measured using the ABTS activity assay with rGLOX from *P.pastoris* and *T.reesei* with each buffer having one to two overlapping points as control points. From the obtained results (Figure 13) it is visible that profiles from both hosts are quite similar with a rather narrow pH range (pH 5.0 - 7.0) for enzyme activity and a pH optimum at pH 6.0. They coincide with the results published by Kersten and Kirk (Kersten and Kirk, 1987) using the native GLOX from *P.chryso sporium* and with the results obtained by measuring rGLOX activity of *Pycnoporus cinnabarinus* heterologously expressed in *Aspergillus niger* (Daou et al., 2016). Deviations occur in relation to the results published for rGLOX from *P. chryso sporium* heterologously expressed in *P.pastoris* (Son et al., 2012). In this publication, pH 5.0 is stated as the optimal pH value and the deviation in the results may be due to the use of MnP instead of HRP and the use of buffers of different compositions. High standard deviations in samples of MOPS buffer (Figure 13) may be a consequence of ABTS radical instability in "Good buffers".

#### 4.2.4. Copper loading - Zincon assay

Formazan dye Zincon has long been known as an excellent colorimetric reagent for the detection of zinc and copper ions in aqueous solutions. As a member of enzymes class CRO, GLOX is a metalloenzyme containing one copper metal ion in its active site, which is required for its full activity. To determine the amount of copper present in the enzyme, Zincon assay was used.

In order to be able to determine the concentration of copper, it is necessary to make a calibration curve, which was made using  $\text{CuCl}_2$  (Figure 14).

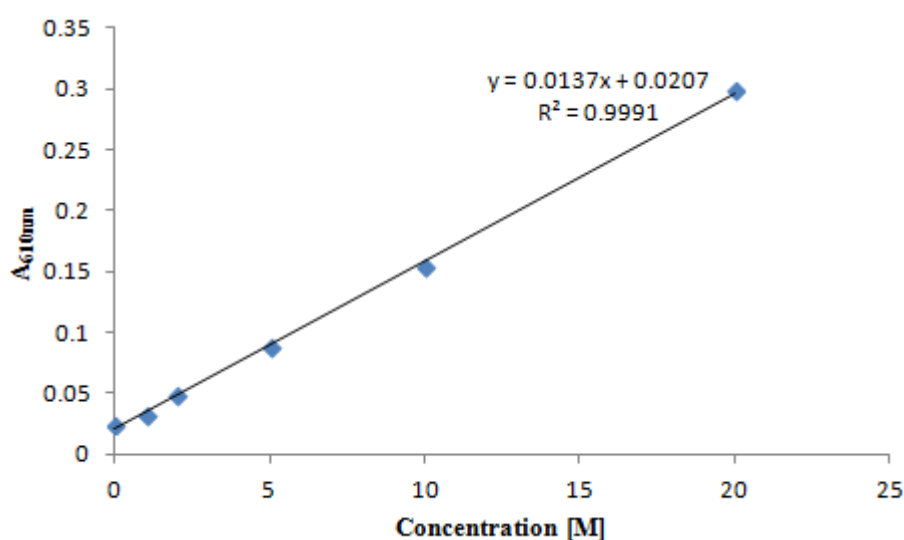


Figure 14. Calibration curve generated with  $\text{CuCl}_2$

To examine the protein concentration present in a sample solution, in addition to 610 nm, absorption was simultaneously measured at 280 nm, too. From the obtained absorption values, the present concentrations of the proteins and copper ions were calculated using the Lambert-Beer law.

Table 14. Zincon assay data

Sample	Absorbance		Protein concentration	$\text{Cu}^{2+}$ concentration	Ratio
	$A_{280\text{nm}}$	$A_{610\text{nm}}$	[ $\mu\text{M}$ ]	[ $\mu\text{M}$ ]	[%]
<i>P.pastoris</i>	0.239	0.082	6.765	4.552	65.9
<i>T.reesei</i>	0.356	0.092	10.081	5.349	51.7

To be active, GLOX needs and can contain only one copper in its active site (Whittaker *et al.*, 1996). Relying on this data that previous studies confirmed, obtained values (protein and copper concentrations) were put in a ratio to calculate the percentage of active enzyme produced in *P.pastoris* and *T.reesei*. Ratios shows that 65.9% of rGLOX produced in *P. pastoris* is active and 51.7% of rGLOX from *T. reesei*. These results (Table 14) are quite similar with copper loading determined by Whittaker in 1999 (Whittaker *et al.*, 1999), although in this paper as method of detection atomic absorption spectroscopy was used.

#### 4.2.5. rGLOX reconstitution with Cu<sup>2+</sup>

Philip J. Kersten has reported that after GLOX was purified without Cu<sup>2+</sup> in the buffers, a great loss of activity occurred, but it was partially regained by incubation with 1 mM Cu<sup>2+</sup> solution in 50 mM sodium 2,2-dimethylsuccinate buffer (pH 6.0) at 25 °C. It resulted with 5-fold increase in activity in 1h with 50% of this activation occurring within the first 8 min (Kersten, 1990).

In this study, the calculated ratios showed that a bit more than half of the enzyme preparation was active, which leaves 34 – 48% of inactive enzyme. For that reason, an attempt for rGLOX reconstitution was made. Reconstitution was carried out in a several different conditions (Table 10) with activity measurements after 3 and 23 h from the beginning of the incubation.

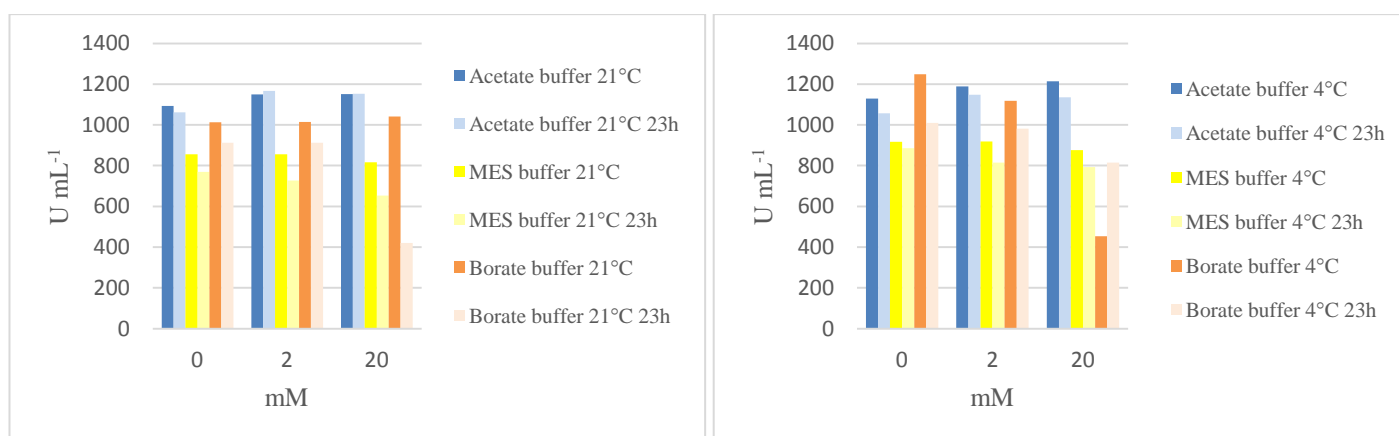


Figure 15. Enzyme activity at 21°C and 4°C

Nevertheless, the reconstitution attempt was not successful. Enzyme activity remained the same or slightly decreased, but under any circumstances it did not increase (Figure 15).

#### 4.2.6. Substrate screening

The substrate specificity of GLOX is broad, with simple aldehyde,  $\alpha$ -hydroxycarbonyl and  $\alpha$ -dicarbonyl compounds supporting activity. Kersten and Cullen (Kersten and Cullen, 1993) showed that GLOX acts primarily on sugar metabolites such as methylglyoxal and glyoxal, but also was found to act on lignin degradation products such as glycoaldehyde. Accordingly, the screening of several different compounds listed in Table 6 was performed and all potential substrates were tested in a final concentration of 10 mM.

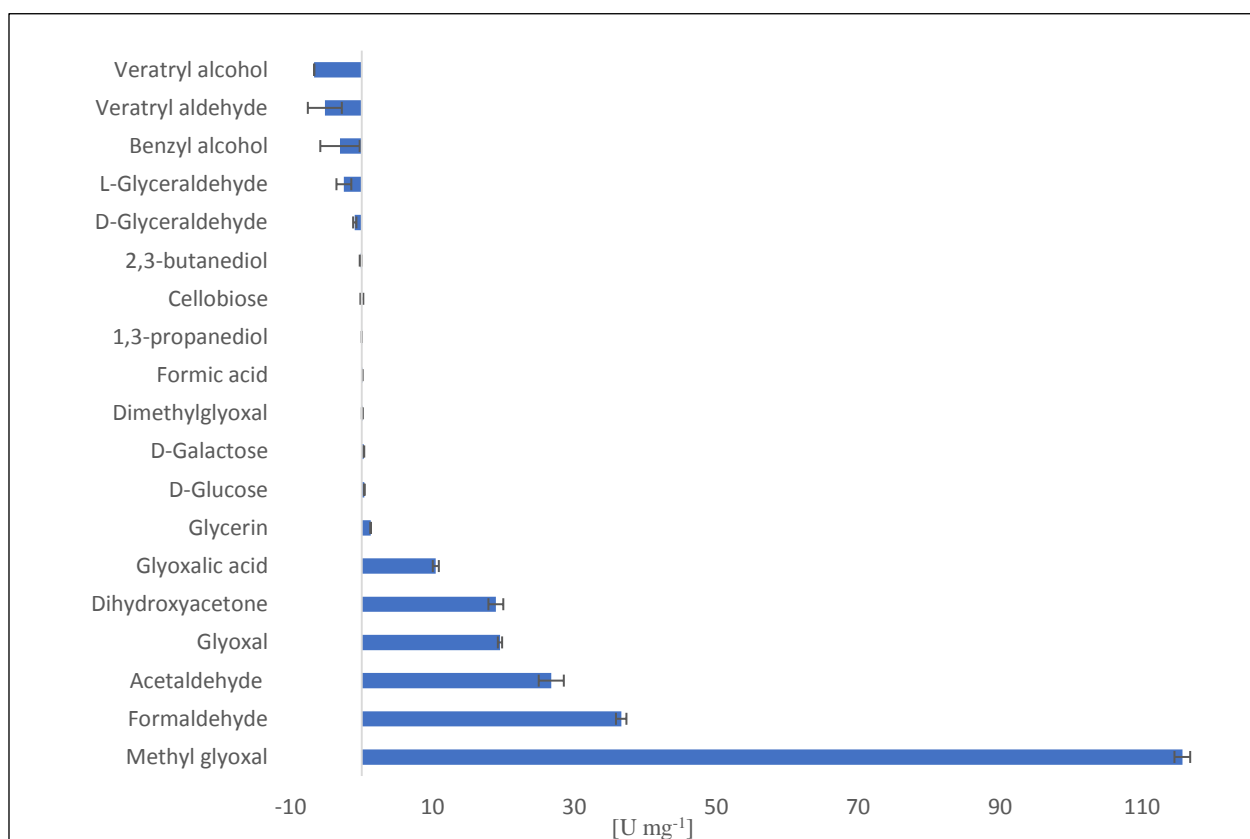


Figure 16. Screened substrates

The obtained screening results (Figure 16) confirmed previously reported results from Kersten and Kirk (Kersten and Kirk, 1987), indicating that the highest activity was reached with methylglyoxal. As in this study, Kersten and Kirk also used GLOX isolated from *P.chryso sporium*, but deviations occurred when the results were compared with the results obtained from GLOX of *Pycnoporus cinnabarinus* (Daou et al., 2016). Two GLOXs of *P.cinnabarinus* heterologously produced in *A.niger*, best specific activity have shown with glyoxalic acid followed by methyl glyoxal, while specific activity of GLOX isolated from

*P.chrysosporium* for glyoxalic acid is not that significant (Figure 16, Kersten and Kirk, 1987). That proves the difference between the substrate specificity and the alternative mechanism existing in a different fungi. In all previously mentioned studies, the inability of rGLOX to oxidize sugars and alcohols (Figure 16) have been shown and negative activity of certain samples, as previously described in chapter 4.2.2., is likely a consequence of high sensitivity and instability of ABTS radical in certain solutions.

### **4.3. ACTIVATOR ASSAY ESTABLISHMENT**

For the purpose of testing numerous compounds as a potential activators of GLOX, a new activity assay needed to be established. The reason why ABTS activity assay was not suitable for that purpose is that active HRP uses ABTS as an electron donor during the reduction of hydrogen peroxide to water. The resultant product is ABTS radical and as it has been shown before, ABTS radical itself activates rGLOX making it difficult to use as a GLOX-activator-screening system. For this reason, the main intention was to establish an assay in which the HRP reaction product will not interfere with GLOX.

#### **4.3.1. TMB assay**

The attempt to establish the TMB assay was based on the standard ABTS assay used throughout the study. The assay was adapted by using 3,3',5,5'-Tetramethylbenzidine (TMB) as a HRP substrate instead of ABTS reagent. The main challenge was to find an appropriate final concentration of TMB at which no precipitants would occur because, with its appearance, it is not possible to measure the absorbance reliably. This was achieved with a final concentration of 100  $\mu$ M TMB. As a proven activator (Figure 11), ABTS radical solution (10  $\mu$ M) was used and as a negative control an activator-free sample was run.

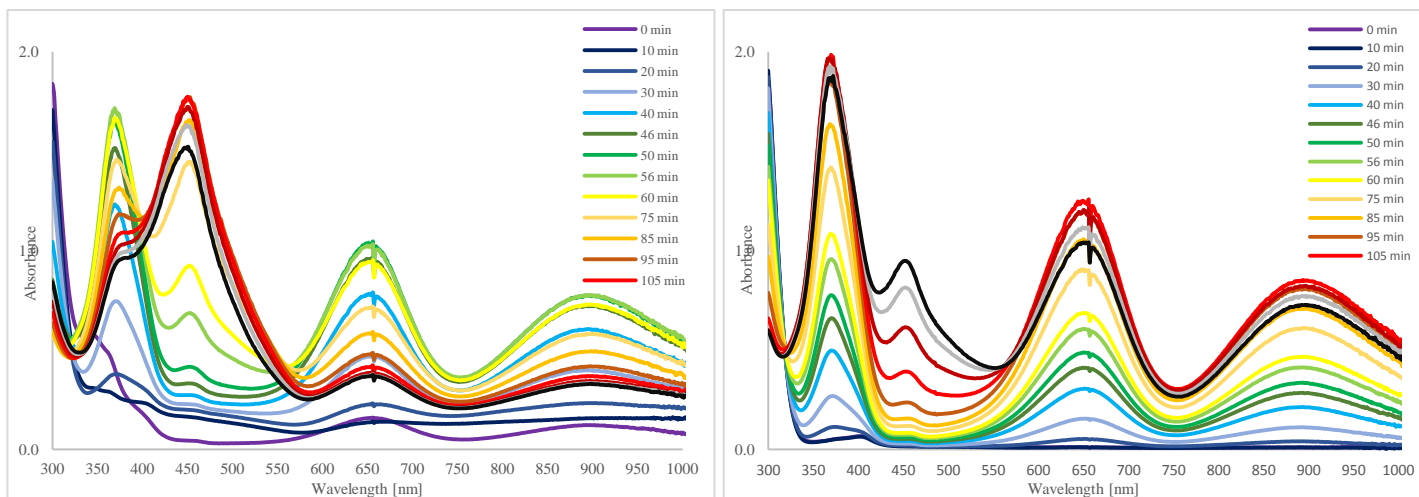


Figure 17. TMB assay with ABTS radical (sample) and without ABTS radical (negative controle)

The reaction was run at the diode array photometer because of its capability for a whole spectrum detection. In the first half of the reaction, peak growth at 650 nm was observed (Figure 17) and after 50-60 minutes, the maximum was reached. Shortly after, the peak started to decrease while a new peak at 450 nm was increasing, which shows the formation of a second product.

Due to the previous studies, the oxidation of TMB takes place in two stages (one-electron oxidation and two-electron oxidation), yielding products with different colors (blue and yellow). As a product of the one-electron oxidation, a blue-color product (cation free radical) is formed, which is detected at 650 nm, while a second-electron oxidation product is a yellow-colored diimine with absorption at 450 nm. Reaching the maximum absorption at 650 nm (after 50-60 minutes, Figure 17 with ABTS radical) corresponds to the molar correlation of  $\frac{1}{2}$  mol of  $H_2O_2$  / 1 mol of TMB and the second stage of oxidation ends when approximately equimolar concentrations of  $H_2O_2$  and substrate are reached, after which the concentration of yellow product remains constant (Josephy et al., 1982).

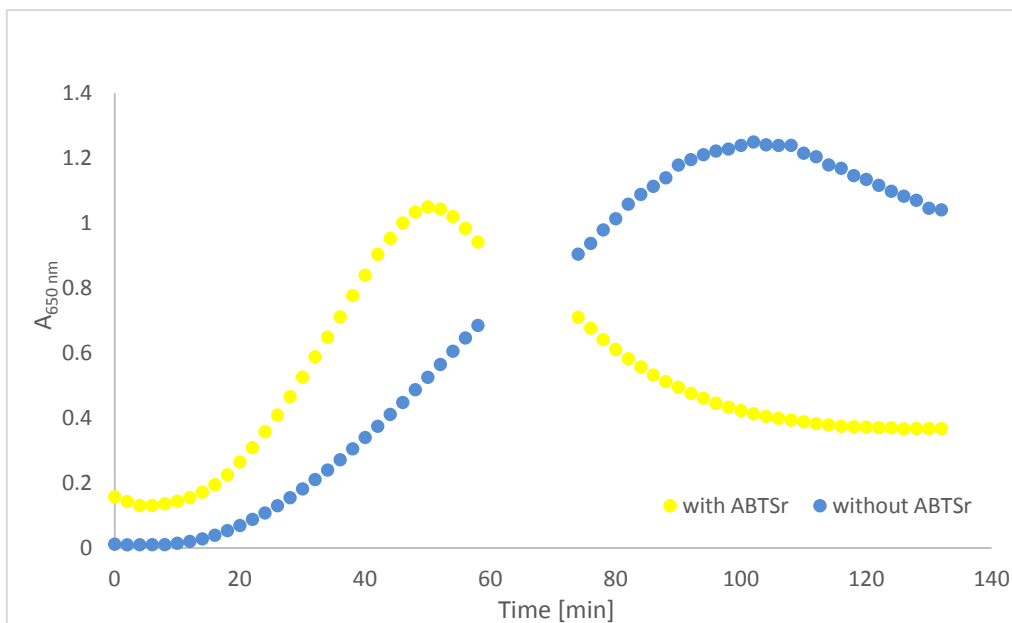


Figure 18. TMB assay time drive

As a proven activator, ABTS radical was used and the absence of lag phase was expected in that sample. According to the obtained results (Figure 18) the lag phase is present and it is accompanied by a noticeable decrease at the very beginning of the reaction (first 2-3 min). The instability of the ABTS radical in the used "Good buffer" and concomitant oxidation of GLOX by ABTS radical causing its reduction, could lead to a decrease of the absorption signal.

In the negative control sample, the addition of an activator was omitted so no reaction should have taken place. The obtained results show (Figure 18) that the reaction proceeded, only much slower. Because of these disadvantages, presence of the lag phase in a sample with activator and slow, but still ongoing reaction in a sample without any activator, TMB has not proven to be a suitable reagent for a plausible activity assay. To know how TMB exactly interferes with GLOX and what causes the obtained results, further and more detailed investigations are necessary.

#### 4.3.2. Amplex red assay

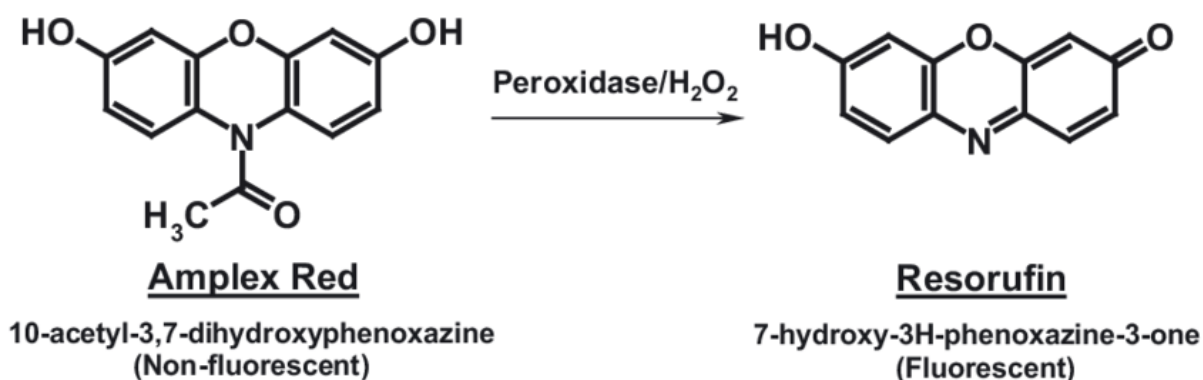


Figure 19. Oxidation of non-fluorescent Amplex Red into highly fluorescent resorufin using hydrogen peroxide and peroxidase (Kulys, 2008)

Amplex Red reagent is a colorless HRP substrate that reacts with hydrogen peroxide to produce resorufin. Resorufin is a highly fluorescent compound that can be detected spectrophotometrically at 571 nm. In order to prove that resorufin does not have any activating effect on rGLOX, ABTS activity assay was performed using  $H_2O_2$  and ABTS radical as a positive control and an activator-free sample as a negative control. Because of the presence of lag phase with the same duration as in the negative control, the obtained results (Figure 19) show that resorufin has no effect on rGLOX.

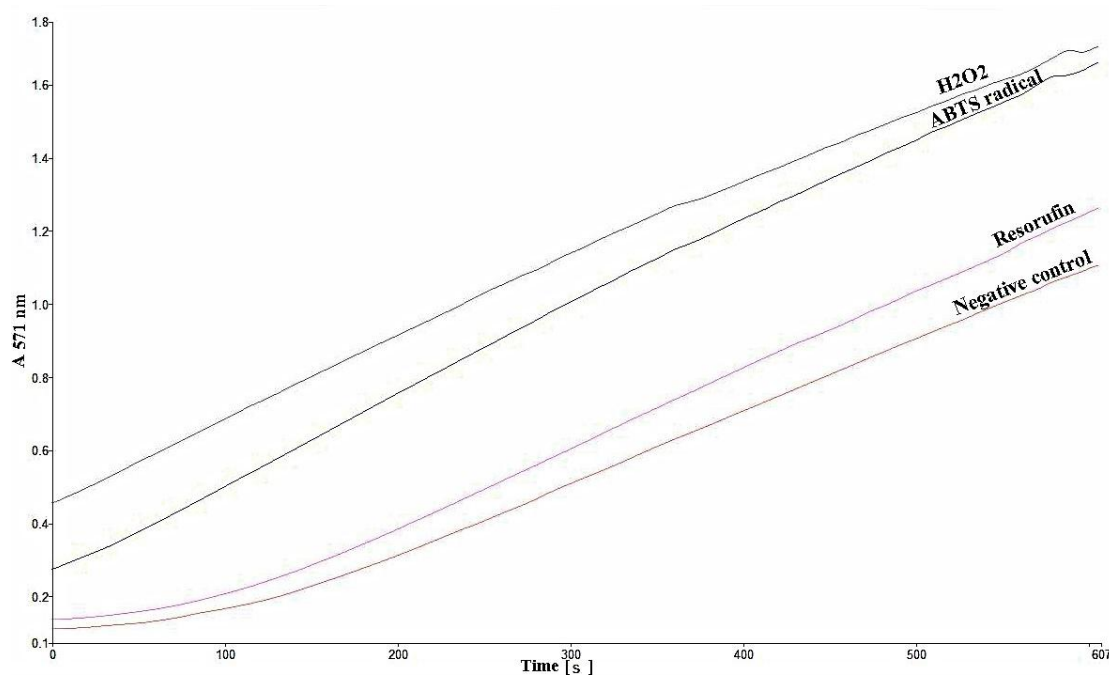


Figure 20. Results of an activity assay performed with resorufin



Despite the proven fact that resorufin is not activating GLOX, the establishment of an Amplex red assay was not successful. The main reason for the failure was resorufin's instability at pH 6.0, detected by a rapid color fading in a short time period. pH value suitable for resorufin's stability is pH 7.0, but at this pH activity of rGLOX decreases dramatically and therefore, the Amplex red was also not suitable for an assay establishment.

#### 4.3.3. 2,6-DMP assay

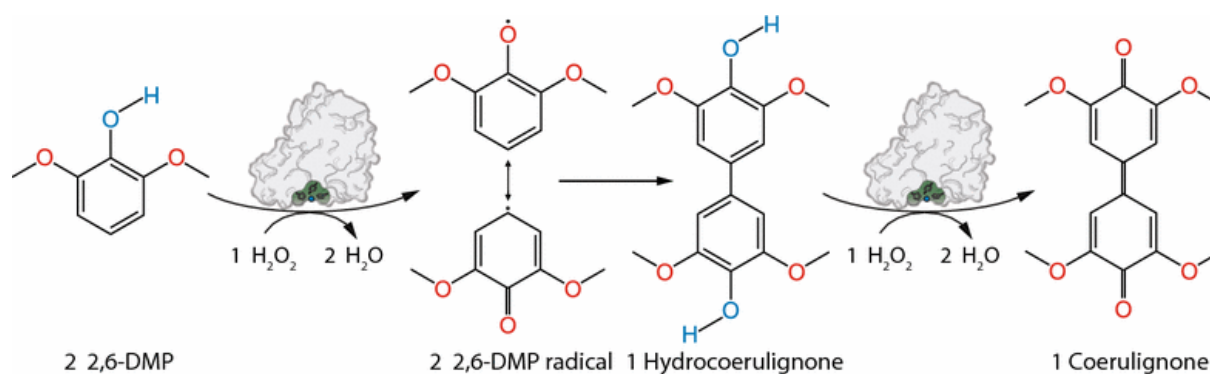


Figure 21. 2,6-DMP oxidation (Breslmayr et al., 2018)

The last attempt to establish a new assay was with 2,6-dimethoxyphenol (2,6-DMP). HRP is oxidizing 2,6-DMP into coerolignone, a highly colored product (orange), using two molecules of  $\text{H}_2\text{O}_2$ . The formation of coerulignone involves two steps and starts with the oxidation of two 2,6-DMP molecules, spontaneously dimerizing into a dimer (hydrocoerulignone). In the second step, the formed hydrocoerulignone molecule is oxidized to the chromogenic compound coerulignone, whose absorption can be detected at 469 nm (Breslmayr et al., 2019).

During the measurement, after the addition of  $\text{H}_2\text{O}_2$ , in a period of 10-20 min, a great loss of color was observed. This may be a consequence of background reaction (coerolignone  $\rightarrow$  hydrocoerolignone  $\rightarrow$  2,6-DMP) due coerolignone instability at the assay conditions. For the reasons stated above, unfortunately, 2,6-DMP was also not suitable for the assay establishment.

#### 4.4. rGLOX ACTIVATION

Due to the previous studies GLOX is reversibly inactivated during the purification, but can be reactivated when coupled to peroxidase system (LiP and HRP) (Kurek and Kersten, 1995). Since it has been reported that rGLOX is activated by the products from peroxidase oxidation, one goal in this thesis was to identify potential activators of rGLOX. Due to the GLOX participation in the process of lignocellulose degradation, the compounds that potentially can occur during this process in its natural environment were tested first.

Despite the proven activation potential of ABTS radical, because of the unsuccessful attempts to establish an assay that will serve to detect activators without the usage of ABTS reagent, for further testing the regular ABTS activity assay was used. Determining whether a particular molecule activates rGLOX or does not activate it, was based on occurrence and comparison of a lag phase.

##### 4.4.1. Quinones

Table 15. Quinones tested for activation of GLOX (Kracher et al., 2016)

Quinone	$E^{\frac{1}{2}}$ (mV vs. SHE)
Tetrafluoro-p-benzoquinone	706
Methoxy-1,4-benzoquinone	144
2,6-Dimethyl-1,4-benzoquinone	148
2,6-Dimethoxy-1,4-benzoquinone	225

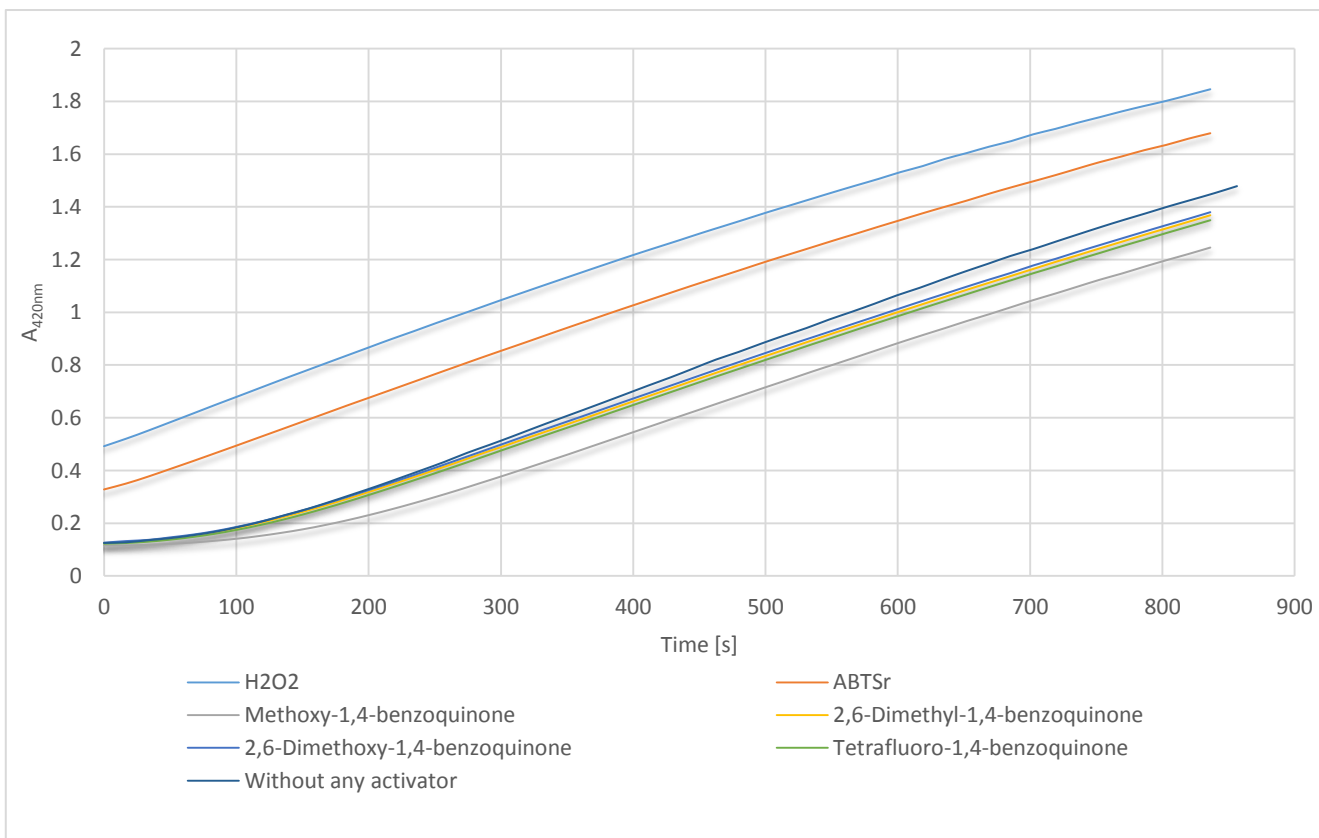


Figure 22. GLOX activity measurements testing various quinones as activators

In the measurements  $H_2O_2$  and ABTS radical were used as positive controls and a sample without any activator as a negative control. Due to the presence of lag phase in all samples and almost in the same duration as in the sample of negative control, it can be said that quinones do not have the ability to activate rGLOX. The reason may be that the reduction potentials of quinones (Table 14) are lower than the redox potential of rGLOX ( $E^{1/2} = 0.64$  V vs. NHE, pH 7.0) (Whittaker et al., 1996), which is why they were unable to transfer electrons to rGLOX, its active state being the oxidized state.

#### 4.4.2. Phenoxy radicals

Despite the fact that rGLOX activation by the lignin peroxidase system with veratryl alcohol has been proven by measuring the  $O_2$  consumption during the reaction (Kersten, 1990), due to the inability of the laccase to oxidize veratryl alcohol, this compound could not be tested with the spectrophotometric assay used in this thesis. All other phenoxy radicals from Table 7. were successfully generated using the laccase from *Botrytis aclada*. In every

compound solution 5-fold excess of laccase was added and after completion of the oxidation process, the enzyme was removed using the Amicon centrifugal filters.

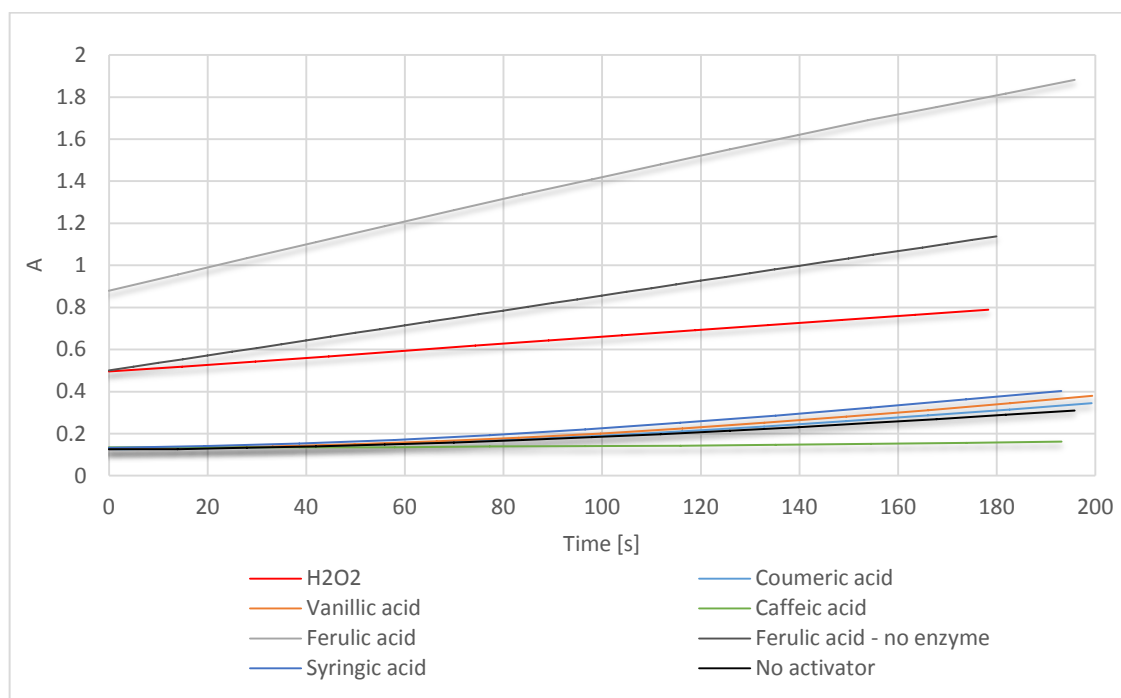


Figure 23. GLOX activity measurements testing various phenoxy radicals as activators

From tested acids, ferulic acid stood out as an activator more potent than  $H_2O_2$ . Consequently, the reaction was repeated without the addition of the enzyme where the activity was still higher than with the  $H_2O_2$ . From the obtained results it can be concluded that ferulic acid is highly reactive with the ABTS solution itself, which is why results are not reliable and the testing cannot be performed using the ABTS activity assay. Also, as evidenced by the presence of the lag phase in a duration equal to the sample without any activator, none of the other tested compounds proved to be a successful activator of rGLOX (Figure 23).

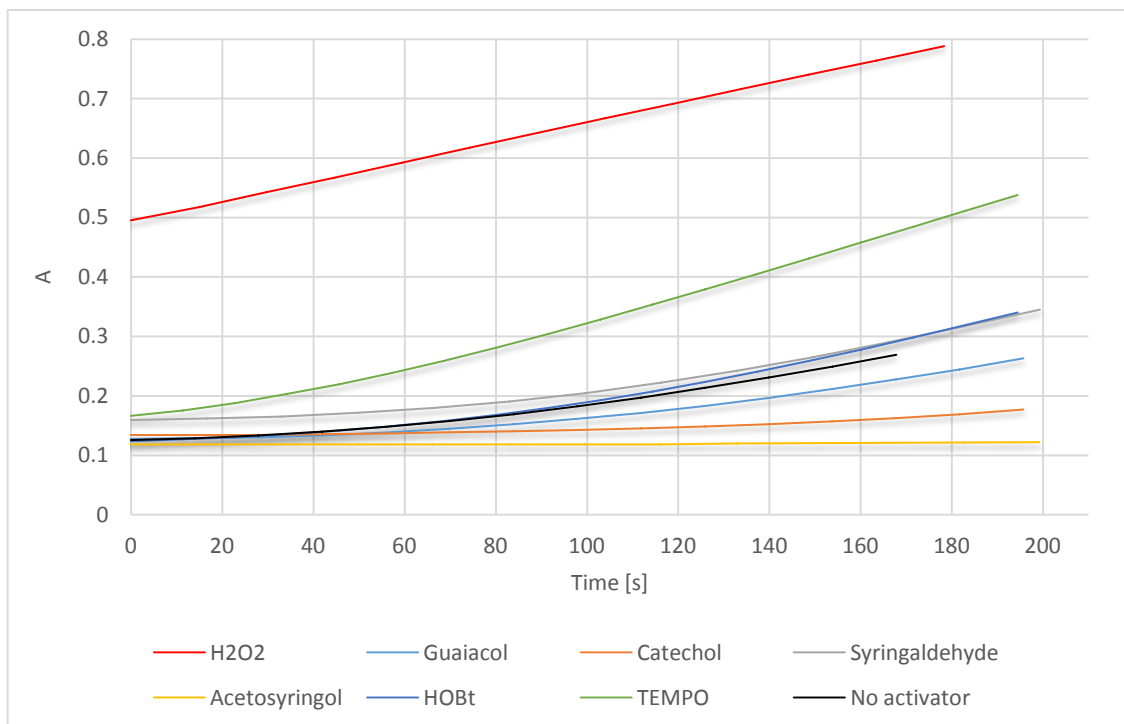


Figure 24. GLOX activity measurements testing various phenoxy radicals as activators

From the rest of the tested compounds, TEMPO stands out with a slightly higher activation ability, but as in the case of other compounds, the lag phase is still present, so the overall activating effect is not considered significant (Figure 24).

## 5. CONCLUSIONS

Relying on the results obtained and processed in this thesis, the following conclusions can be drawn:

1. In the fermentation medium from native organism *Phanerochaete chrysosporium*, glyoxal oxidase and other oxidoreductases could not be detected, but the presence of different hydrolases was determined, so they were purified and stored as an enzyme cocktail of *P. chrysosporium*.
2. The pH profile of rGLOX was measured for enzyme samples from both hosts, *Pichia pastoris* and *Trichoderma reesei*, thereby determining an optimum pH value at pH 6.0 in both cases.
3. An ABTS radical and phenoxy radicals were successfully generated using the laccase from *Botrytis aclada*.
4. ABTS radical impact on rGLOX activity was investigated and activation ability was determined. Also, its high sensitivity and instability dependent on the buffer composition and strong illumination has been discovered.
5. In the GLOX samples from both expression hosts, only 52-66% of the enzymes were found to contain a copper ion required for full activity in their active site. An attempt to reconstitute the enzyme, loading it with copper and thus increasing the percentage of active enzyme, unfortunately failed.
6. GLOX catalyzes the oxidation of a number of simple aldehydes and  $\alpha$ -hydroxy carbonyl compounds, but it is not oxidizing sugars. Among the different substrates that have been tested, the highest activity was found with methylglyoxal.
7. Due to the proven activation ability of ABTS radical for rGLOX, in order to test potential activators, an attempt to establish a new assay independent from ABTS was made. Unfortunately, this establishment did not complete successfully and for further use ABTS activity assay was used. The detection of potential activation ability was based on the occurrence and duration of the lag phase.

8. Different types of chemical compounds present during the lignin degradation process have been tested as a potential activators of rGLOX, but unfortunately no activation ability has been identified.

## 6. REFERENCES

1. Alonso, D.M., Bond, J.Q., Dumesic, J.A. (2010) Catalytic conversion of biomass to biofuels. *Green Chem.* 12, 1493–1513.
2. Andlar, M., Rezić, T., Mardetko, N., Kracher, D., Ludwig, R., Šantek, B. (2018) Lignocellulose degradation: An overview of fungi and fungal enzymes involved in lignocellulose degradation. *Eng. Life Sci.* 18, 768–778.
3. Breslmayr, E., Daly, S., Požgajčić, A., Chang, H., Rezić, T., Oostenbrink, C., Ludwig, R. (2019) Biotechnology for Biofuels Improved spectrophotometric assay for lytic polysaccharide monooxygenase. *Biotechnol. Biofuels* 1–12.
4. Breslmayr, E., Hanžek, M., Hanrahan, A., Leitner, C., Kittl, R., Šantek, B., Oostenbrink, C., Ludwig, R. (2018) Biotechnology for Biofuels A fast and sensitive activity assay for lytic polysaccharide monooxygenase. *Biotechnol. Biofuels* 1–13.
5. Daou, M., Faulds, C.B. (2017) Glyoxal oxidases: their nature and properties. *World J. Microbiol. Biotechnol.* 33, 1–11.
6. Daou, M., Piumi, F., Cullen, D., Record, E., Faulds, B. (2016) Heterologous Production and Characterization of Two Glyoxal Oxidases from *Pycnoporus cinnabarinus* 82, 4867–4875.
7. Den, W., Sharma, V.K., Lee, M., Nadadur, G., Varma, R.S. (2018) Lignocellulosic biomass transformations via greener oxidative pretreatment processes: Access to energy and value added chemicals. *Front. Chem.* 6, 1–23.
8. Esposito, D., Antonietti, M. (2015) Redefining biorefinery: the search for unconventional building blocks for materials. *Chem. Soc. Rev.* 44, 5821–5835.
9. Henrich, E., Dahmen, N., Dinjus, E. (2015) The Role of Biomass in a Future World without Fossil Fuels 1667–1685.



10. Horn, S.J., Vaaje-kolstad, G., Westereng, B., Eijsink, V.G. (2012) Novel enzymes for the degradation of cellulose. *Biotechnol Biofuels*. *Biotechnol. Biofuels* 5, 45.
11. Janušić, V., Ćurić, D., Krička, T., Voća, N., Matin, A. (2008) Pretreatment technologies in bioethanol production from lignocellulosic biomass. *Poljoprivreda* 14.
12. Janusz, G., Pawlik, A., Sulej, J., Świdorska-Burek, U., Jarosz-Wilkolazka, A., Paszczyński, A. (2017) Lignin degradation: Microorganisms, enzymes involved, genomes analysis and evolution. *FEMS Microbiol. Rev.* 41, 941–962.
13. Josephy, D., Eling, T., Mason, R. (1982) The Horseradish Peroxidase-catalyzed Oxidation of 3,5,3',5'- Tetramethylbenzidine. *J. Biol. Chem.* 257, 3669–3675.
14. Kersten, P.J. (1990) Glyoxal oxidase of *Phanerochaete chrysosporium*: Its characterization and activation by lignin peroxidase. *Proc. Natl. Acad. Sci. U. S. A.* 87, 2936–2940.
15. Kersten, P.J., Cullen, D. (1993) Cloning and characterization of a cDNA encoding glyoxal oxidase, a H<sub>2</sub>O<sub>2</sub>- producing enzyme from the lignin-degrading basidiomycete *Phanerochaete chrysosporium*. *Proc. Natl. Acad. Sci. U. S. A.* 90, 7411–7413.
16. Kersten, P.J., Kirk, T.K. (1987) Involvement of a new enzyme, glyoxal oxidase, in extracellular H<sub>2</sub>O<sub>2</sub> production by *Phanerochaete chrysosporium*. *J. Bacteriol.* 169, 2195–2201.
17. Kovačić, Đ. (2017) Razvoj procesa predobrade lignoceluloznih materijala toplinom i električnim poljem u svrhu primjene u proizvodnji bioplina anaerobnom kodigestijom s goveđom gnjojovkom (doktorska disertacija), Sveučilište J.J. Strossmayera u Osijeku & Institut Ruđer Bošković, Osijek.
18. Kracher, D., Scheiblbrandner, S., Felice, A.K.G., Breslmayr, E., Preims, M., Ludwicka, K., Haltrich, D., Eijsink, V.G.H., Ludwig, R. (2016) Extracellular electron

- transfer systems fuel cellulose oxidative degradation. *Science* (80-. ). 352, 1098–1101.
19. Kulys, J. (2008) Kinetic study of peroxidase-catalyzed oxidation of 1-hydroxypyrene . Development of a nanomolar hydrogen peroxide detection system 3.
  20. Leuthner, Birgitta & Aichinger, C & Oehmen, E & Koopmann, Edda & Mueller, O. & Mueller, Philip & Kahmann, Regine & Bolker, M. & Schreier, Peter. (2005) A H<sub>2</sub>O<sub>2</sub>-producing glyoxal oxidase is required for filamentous growth and pathogenicity in *Ustilago maydis*. *Molecular Genetics and Genomics*, v.272, 639-650 .
  21. Kurek, B., Kersten, P.J. (1995) Physiological regulation of glyoxal oxidase from *Phanerochaete chrysosporium* by peroxidase systems. *Enzyme Microb. Technol.* 17, 751–756.
  22. Riley, R., Salamov, A.A., Brown, D.W., Nagy, L.G., Floudas, D., Held, B.W., Grigoriev, I. V, (2014) Extensive sampling of basidiomycete genomes demonstrates inadequacy of the white-rot / brown-rot paradigm for wood decay fungi.
  23. Rubin, E.M. (2008) Genomics of cellulosic biofuels. *Nature* 454, 841–845.
  24. Säbel, C.E., Neureuther, J.M., Siemann, S. (2010) A spectrophotometric method for the determination of zinc, copper, and cobalt ions in metalloproteins using Zincon. *Anal. Biochem.* 397, 218–226.
  25. Son, Y., Kim, H., Thiyagarajan, S., Xu, J.J., Park, S. (2012) Heterologous Expression of *Phanerochaete chrysosporium* Glyoxal Oxidase and its Application for the Coupled Reaction with Manganese Peroxidase to Decolorize Malachite Green 40, 258–262.
  26. Van Wyk, J.P.H. (2011) Biowaste as a resource for bioproduct development. *Environ. Earth Sci.* 19, 875–883.
  27. Whittaker, M.M., Kersten, P.J., Nakamura, N., Sanders-Loehr, J., Schweizer, E.S., Whittaker, J.W. (1996) Glyoxal oxidase from *Phanerochaete chrysosporium* is a new

radical-copper oxidase. *J. Biol. Chem.* 271, 681–687.

28. Whittaker, J.W. (2003) Free radical catalysis by galactose oxidase. *Chem. Rev.* 103, 6, 2347-2364.

## STATEMENT OF ORIGINALITY

This is to certify, that the intellectual content of this thesis is the product of my own independent and original work and that all the sources used in preparing this thesis have been duly acknowledged.

*Matea Zrilić*

Matea Zrilić